In: Trends in Quantum Gravity Research
Editor: David C. Moore, pp. 65-107
ISBN: 1-59454-670-3

Chapter 2

QUANTUM STATES OF NEUTRONS IN THE EARTH'S GRAVITATIONAL FIELD: STATE OF THE ART, APPLICATIONS, PERSPECTIVES

V.V. Nesvizhevsky[1] and K.V. Protasov[2]
[1] Institut Laue-Langevin, Grenoble, France
[2] Laboratoire de Physique Subatomique et de Cosmologie,
IN3P3-CNRS-UJF, Grenoble

Abstract

Gravitationally bound quantum states of matter were observed for the first time thanks to the unique properties of ultra-cold neutrons (UCN). The neutrons were allowed to fall towards a horizontal mirror which, together with the Earth's gravitational field, provided the necessary confining potential well. In this paper we discuss the current status of the experiment, as well as possible improvements: the integral and differential measuring modes; the flow-through and storage measuring modes; resonance transitions between the quantum states in the gravitational field or between magnetically split sub-levels of a gravitational quantum state.

This phenomenon and the related experimental techniques could be applied to various domains ranging from the physics of elementary particles and fields (for instance, spin-independent or spin-dependent short-range fundamental forces or the search for a non-zero neutron electric charge) to surface studies (for instance, the distribution of hydrogen in/above the surface of solids or liquids, or thin films on the surface) and the foundations of quantum mechanics (for instance, loss of quantum coherence, quantum-mechanical localization or experiments using the very long path of UCN matter waves in medium and in wave-guides).

In the present article we focus on transitions between the quantum states of neutrons in the gravitational field, consider the characteristic parameters of the problem and examine various methods for producing such transitions. We also analyze the feasibility of experiments with these quantum transitions and their optimization with respect to particular physical goals.

1 Introduction

The quantum motion of a particle with mass m in the terrestrial gravitational field and the acceleration g above an ideal horizontal mirror is a well-known problem in quantum mechanics which allows an analytic solution involving special functions known as Airy functions. The solutions of the corresponding Schrödinger equation with linear potential were discovered in 1920th [1] and can be found in major textbooks on quantum mechanics [2–7]. For a long time, this problem was considered only as a good theoretical exercise in quantum mechanics. The main obstacle for observing these quantum states experimentally was the extreme weakness of the gravitational interaction with respect to electromagnetic one, which meant that the latter could produce considerable false effects. In order to overcome this difficulty, an electrically neutral long-life particle (or quantum system) must be used for which an interaction with a mirror can be considered as an ideal total reflection. Ultracold neutrons (UCN) were discussed in this respect in refs. [8, 9]. UCN [10, 11] represent an extremely small initial part of total neutron flux. A reactor with very high neutron flux is therefore required. These quantum states were observed and investigated for the first time in a series of experiments [12–15] performed at the high-flux reactor at the Institut Laue-Langevin in Grenoble. Other quantum optics phenomena invetsigated with neutrons are presented in ref. [16].

To observe the gravitationally bound states, two experimental techniques were used. The first one, the so-called "integral" flow-through mode, is a measurement of the neutron flux through a narrow horizontal slit between a mirror below and an absorber/scatterer above it, which is used to scan the neutron density distribution above the mirror. This experimental technique allowed us to observe, for the first time, the non-continuous (discrete) behavior of the neutron flux. This observation was interpreted as being due to quantum states of neutrons corresponding to their vertical motion in the slit. Another, more sophisticated, so-called "differential" mode is based on specially developed position-sensitive neutron detectors with a very high spatial resolution, which made it possible to begin more detailed studies of this system and, in particular, to measure the spatial distributions of neutrons as a function of their height above a mirror (the square of the neutron wave function).

The present article does not claim to give an exhaustive overview of the different, rapidly developing applications of this beautiful phenomenon; it simply focuses on areas of particular interest to our research at present. In section 2, we start by giving a brief presentation of the phenomenon itself and in section 3 we describe the first experiment in which the ground quantum state was observed. Section 4 is devoted to a discussion of the "differential" measuring mode. Some of the interesting consequences of this experiment in different domains of physics (such as the search for exotic particles and spin-independent or spin-dependent short-range fundamental interactions; foundations of quantum mechanics) are discussed in section 5. Particular attention is paid to further developments of this experiment. In section 6, we present for the first time a feasibility analysis and theoretical description of the observation of resonance transitions between the quantum states. Such transitions could be induced by various interactions: by strong forces (if the mechanical oscillations of a bottom mirror are applied with a frequency corresponding to the energy difference between the quantum states), by electromagnetic forces (oscillating magnetic field), or probably even,

at the limit of experimental feasibility, by gravitational forces (oscillating mass in the vicinity of the experimental setup). Some other methodological applications are also discussed.

2 The Properties of the Quantum States of Neutron in the Earth's Gravitational Field

The wave function $\psi(z)$ of the neutron in the Earth's gravitational field satisfies the Schrödinger equation:

$$\frac{\hbar^2}{2m}\frac{d^2\psi(z)}{d^2z}+(E-mgz)\psi(z)=0. \tag{2.1}$$

An ideal mirror at $z=0$ could be approximated as an infinitely high and sharp potential step (infinite potential well). Note that the neutron energy in the lowest quantum state, as will be seen a little later, is of the order of 10^{-12} eV and is much lower than the effective Fermi potential of a mirror, which is close to 10^{-7} eV. The range of increase of this effective potential does not exceed a few nm, which is much shorter than the neutron wavelength in the lowest quantum state ~10 μm. This effective infinite potential gives a zero boundary condition for the wave function:

$$\psi\left(z=0\right)=0. \tag{2.2}$$

The exact analytical solution of equation (1) which is regular at $z=0$, is the so-called Airy-function

$$\psi\left(z\right)=C\,\mathrm{Ai}\left(\frac{z}{z_0}\right). \tag{2.3}$$

Here

$$z_0=\sqrt[3]{\frac{\hbar^2}{2m^2g}} \tag{2.4}$$

represents a characteristic scale of the problem, C being the normalization constant. For neutrons at the Earth's surface the value of z_0 is equal to 5.87 μm. The equation (2.2) imposes the quantization condition:

$$z_n=z_0\lambda_n \tag{2.5}$$

where λ_n are zeros of the Airy function. They define the quantum energies:

$$E_n = mgz_0\lambda_n . \tag{2.6}$$

For the 4 lowest quantum states they are equal to:

$$\lambda_n = \{2.34, 4.09, 5.52, 6.79, \ldots\} \tag{2.7}$$

and for the corresponding energies, we obtain:

$$E_n = \{1.4, 2.5, 3.3, 4.1, \ldots\} \text{ peV}. \tag{2.8}$$

It is useful to obtain an approximate quasi-classical solution of this problem [2–4,7]. This approximation is known to be valid, for this problem, with a very high accuracy, which is of the order of 1% even for the lowest quantum state. In accordance with the Bohr-Sommerfeld formula, the neutron energy in quantum states E_n^{qc} ($n = 1, 2, 3, \ldots$) is equal to:

$$E_n^{\text{qc}} = \sqrt[3]{\left(\frac{9m}{8}\right)\left(\pi\hbar g\left(n-\frac{1}{4}\right)\right)^2} \tag{2.9}$$

The exact energies E_n as well as the approximate quasi-classical values E_n^{qc} have the same property: they depend only on m, g and on the Planck constant $\hbar$, and do not depend on the properties of the mirror.

The simple analytical expression (2.9) shows that the energy of *n*-th state increases as $E_n^{\text{qc}} \sim n^{2/3}$ with increasing n. In other words, the distance between the neighbor levels decreases with increasing n.

In classical mechanics, a neutron with energy E_n in a gravitational field could rise to the maximum height of:

$$z_n = E_n / mg . \tag{2.10}$$

In quantum mechanics, the probability of observing a neutron in *n*-th quantum state with energy E_n at a height *z* is equal to the square of the modulus of its wave function $|\psi_n|^2$ in this quantum state. For the 4 lowest quantum states, neutron residence probability $|\psi_n|^2$ as a function of height above a mirror *z* is presented in Fig. 1 (see [2–6,12,13]). Formally, these functions do not equal zero at any height $z > 0$. However, as soon as a height *z* is greater than some critical value z_n, specific for every *n*-th quantum state and approximately equal to the height of the neutron classical turning point, then the probability of observing a neutron

approaches zero exponentially fast. Such a pure quantum effect of the penetration of neutrons to a classically forbidden region is the tunneling effect. For the 4 lowest quantum states, the values of the classical turning points are equal to:

$$z_n = \{13.7,\ 24.0,\ 32.4,\ 39.9, \ldots\}\ \mu\text{m}. \tag{2.11}$$

An asymptotic expression for the neutron wave functions $\psi_n(z)$ at large heights $z > z_n$ [3, 4, 7] in the classically forbidden region is:

$$\psi_n(\xi_n(z)) \to C_n \xi_n^{-1/4} \exp\left(-\frac{2}{3}\xi_n^{3/2}\right), \tag{2.12}$$

for $\xi_n \to \infty$. Here C_n are known normalization constants and

$$\xi_n = \frac{z_0}{z_n} - \lambda_n . \tag{2.13}$$

As soon as such a height z_n is reached, the neutron wave function $\psi_n(z)$ starts approaching zero exponentially fast.

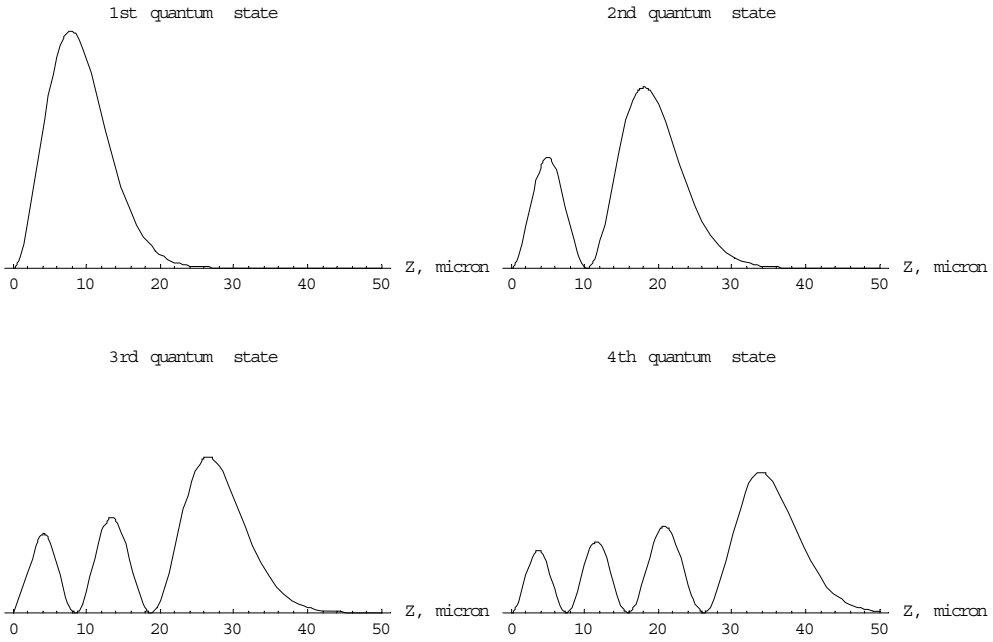

Fig. 1. Neutron presence probability as a function of height above the mirror z for the 1st, 2nd, 3rd and 4th quantum states.

3 Discovery of the Ground Quantum State in the "Integral" Flow-Through Mode

Such a wave-function shape allowed us to propose a method for observing the neutron quantum states. The idea is to measure the neutron transmission through a narrow slit Δz between a horizontal mirror on the bottom and a scatterer/absorber on top (which we shall refer to simply as a scatterer if not explicitly called otherwise). If the scatterer is much higher than the turning point for the corresponding quantum state $\Delta z \gg z_n$, then neutrons pass such a slit without significant losses. When the slit decreases, the neutron wave function $\psi_n(z)$ starts penetrating up to the scatterer and the probability of neutron losses increases. If the slit size is smaller than the characteristic size of the neutron wave function in the lowest quantum state z_1, then such a slit is not transparent for neutrons. Precisely this phenomenon was measured in a series of our recent experiments [12–15].

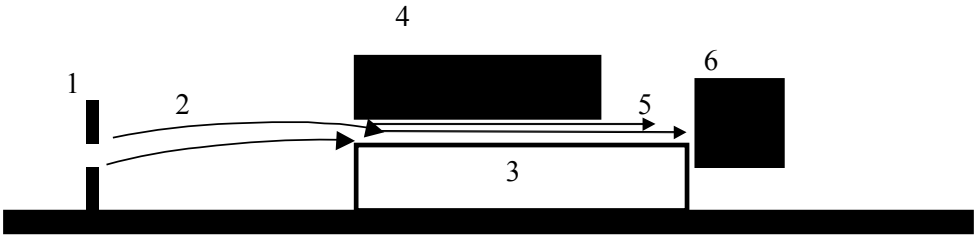

Fig. 2. A basic scheme of the first experiment. From left to right: the vertical bold lines indicate the upper and lower plates of the input collimator (1); the solid arrows correspond to classical neutron trajectories (2) between the input collimator and the entrance slit between the mirror (3, the empty rectangle below) and the scatterer (4, the black rectangle above). The dotted horizontal arrows illustrate the quantum motion of neutrons above the mirror (5), and the black box represents a neutron detector (6). The size of the slit between the mirror and the scatterer could be changed and measured.

A basic scheme of this experiment is presented in Fig. 2. The experiment (also described in ref.[17]) consists of measuring of the neutron flux (with an average velocity of 5–10 m/s) through a slit between a mirror and a scatterer as a function of the slit size. The size of the slit between the mirror and the scatterer can be finely adjusted and precisely measured. The scatterer's surface, while macroscopically smooth and flat, is microscopically rough, with roughness elements measuring in microns. In the classical approximation, one can imagine that this scatterer eliminates those neutrons whose vertical velocity component is sufficient for them to reach its surface. Roughness elements on the scatterer's surface lead to the diffusive (non-specular) reflection of neutrons and, as a result, to the mixing of the vertical and horizontal velocity components. Because the horizontal component of the neutron velocity in our experiment greatly exceeds its vertical component, such mixing leads to multiple successive impacts of neutrons on the scatterer/absorber and, as a result, to the rapid loss of the scattered neutrons. The choice of the absorbing material on the surface of the scatterer/absorber does not play a role, as has been verified experimentally in ref. [15]. Therefore the main mechanism causing the disappearance of neutrons is their scattering on

the rough surface of the scatterer/absorber. This is why it is simply called a scatterer hereafter.

The neutron flux at the front of the experimental setup (in Fig. 2 on the left) is uniform over height and isotropic over angle in the ranges which exceed the slit size and the angular acceptance of the spectrometer respectively by more than one order of magnitude. The spectrum of the horizontal neutron velocity component is shaped by the input collimator with two plates, which can be adjusted independently to a required height. The background caused by external thermal neutrons is suppressed by ''4π shielding'' of the detector. A low-background detector measures the neutron flux at the spectrometer exit. Two discrimination windows in the pulse height spectrum of the ^{4}He detector are set as follows: 1) a "peak" discrimination window corresponds to the narrow peak of the reaction $n + {}^3\mathrm{He} \to t + p$ and provides low background; 2) a much broader range of amplitudes allowes the "counting of all events". This method make it possible to suppress the background efficiently: when the scatterer height is zero and the neutron reactor is "on" then the count rate corresponds, within statistical accuracy, to the detector background measured with the neutron reactor "off".

Ideally, the vertical and horizontal neutron motions are independent. This is valid if the neutrons are reflected specularly from the horizontal mirror and if the influence of the scatterer, or that of any other force, is negligible to those neutrons which penetrate through the slit. If so, the horizontal motion of the neutrons (with an average velocity of 5–10 m/s) is ruled by the classical laws, while in the vertical direction we observe the quantum motion with an effective velocity of a few centimeters per second and with a corresponding energy (2.9) of a few peV (10^{-12} eV). The degree of validity of each condition is not obviously a priori and was therefore verified in related experiments.

The length of the reflecting mirror below the moving neutrons is determined from the energy-time uncertainty relation $\Delta E \Delta t \sim \hbar$, which may seem surprising given the macroscopic scale of the experimental setup. The explanation is that the observation of quantum states is only possible if the energy separation between neighboring levels ($\Delta E_n = E_{n+1} - E_n \sim 1/n^{1/3}$, see (2.8)) is greater (preferably, much greater) than the level width δE. As the quantum number *n* increases, the energy separation ΔE_n between the neighboring levels decreases until the levels ultimately merge into a classical continuum. Clearly, the lower quantum states are simpler and more convenient to measure in methodological terms. As to the width of a quantum state, it is determined by its lifetime or (in our case) by the observation time, i.e. by the neutron's flight time above the mirror. Thus, the length of the mirror is determined by the minimum time of observation of the neutron in a quantum state and should fulfill the condition $\Delta\tau \geq 0.5$ ms. In our experiments, the average value of the horizontal neutron velocity was chosen to be close to 10 m/s or to 5 m/s, implying that a mirror 10 cm in length was long enough.

The vertical scale of the problem, on the other hand, is determined by the momentum-coordinate uncertainty relation $\Delta v_z \cdot \Delta z \sim \hbar / m$. The reason is that the smaller the vertical component of the neutron velocity, the larger the neutron wavelength corresponding to this motion component. However, the classical height to which a neutron can rise in the gravitational field cannot be less than the quantum-mechanical uncertainty in its position, i.e. less than the neutron wavelength. In fact, it is this condition which specifies the lowest bound

state of a neutron in a terrestrial gravitational field. The uncertainty in height is then ~15 μm, whereas the uncertainty in the vertical velocity component is ~1.5 cm/s.

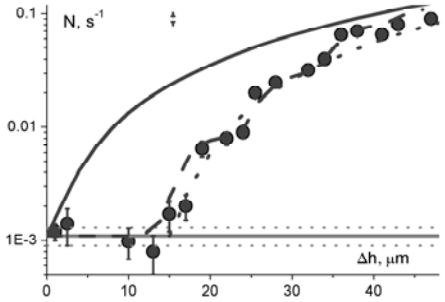

Fig. 3. Neutron flux through a slit between a horizontal mirror and a scatterer above it is given as a function of the distance between them obtained in the first experiment [12,13]. Experimental data are averaged over 2-μm intervals. The dashed line represents quantum-mechanical calculations in which both the level populations and the energy resolution of the experiment are treated as free parameters being determined by the best fit to the experimental data. The solid line corresponds to classical calculations. The dotted line is for a simplified model involving only the lowest quantum state.

The results of the first measurement presented in Fig. 3 (see refs. [12, 13]) differ considerably from the classical dependence and agree well with the quantum-mechanical prediction. In particular, it is firmly established that the slit between the mirror and the scatterer is opaque if the slit is narrower than the spatial extent of the lowest quantum state, which is approximately 15 μm. The dashed line in Fig. 3 shows the results of a quantum-mechanical calculation, in which the level populations and the height (energy) resolution were treated as free parameters. The solid line shows the classical dependence normalized so that, at sufficiently large heights (above 50–100 μm), the experimental results are described well by the line. The dotted line given for illustrative purposes describes a simplified situation with the lowest quantum state alone, i.e. in drawing this line only the uncertainty relation was taken into account. As can be seen from Fig. 3, the statistics and energy resolution of the measurements are still not good enough to detect quantum levels at a wide slit, but the presence of the lowest quantum state is clearly revealed.

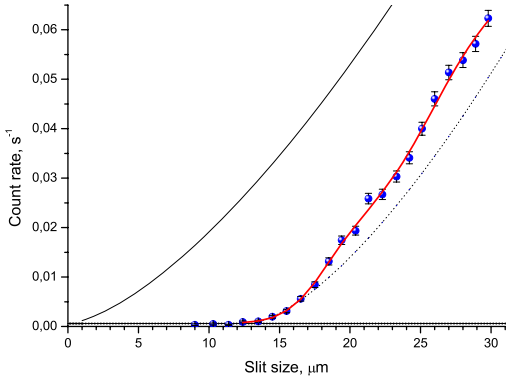

Fig. 4. Neutron flux through a slit between a horizontal mirror and a scatterer above it is given as a function of the distance between them obtained in the second experiment [15].

However, as was shown experimentally (Fig. 4) and explained theoretically in ref. [15], even when the height (energy) resolution and statistics are improved considerably compared to those in refs. [12, 13], further significant improvement of resolution in the "integral" measuring mode presented is scarcely achievable due to one fundamental constraint: the finite sharpness of the dependence on height of the probability of neutron tunneling through the gravitational barrier between the allowed heights for neutrons and the height of the scatterer [15]. As is demonstrated in this article, the neutron flux $F(\Delta z)$ as a function of the scaterrer position Δz above the turning point z_n ($\Delta z > z_n$) can be written within the quasi-classical approximation, for a given level, as:

$$F(\Delta z) \sim \mathrm{Exp}\left(-\alpha \mathrm{Exp}\left(-\frac{4}{3}\left(\frac{\Delta z - z_n}{z_0}\right)^{\frac{3}{2}}\right)\right), \tag{3.1}$$

where z_0 is given in (2.4) and α is a constant. The exponent factor after this constant represents here the probability for the neutron to pass from the classically allowed region to the scatterer/absorber, i.e. the probability of tunneling through the gravitation barrier. This dependence describes the experimental data reasonably well (see Fig. 4) and gives a simple explanation for the existence of intrinsic resolution related to the tunneling effect. Roughly speaking, to resolve experimentally the nearest states $n+1$ and n, the distance $z_{n+1} - z_n$ should be smaller than a characteristic scale of the function (3.1), which is approximately equal to $z_0 = 5.87\ \mu\mathrm{m}$. This condition can be satisfied only for the ground state because even for the first excited state the difference $z_2 - z_1 \approx 8\ \mu\mathrm{m}$ is comparable with z_0.

Nevertheless, the theoretical description of the measured experimental data within the model of the tunneling of neutrons through this gravitational barrier shows reasonable agreement between the extracted parameters of the quantum states and their theoretical prediction. In order to increase the accuracy of this experiment further in the mode which involves scanning the neutron density using a scatterer at various heights, we are working in two directions: First of all, further development [18] of the theoretical description of this experiment could allow us to reduce the theoretical uncertainties in the determination of quantum states parameters to the velev of a few percent. On the other hand, experimental efforts related to improving the accuracy of the absolute positioning of the scatterer [19, 20] would produce a comparable level of accuracy.

To summarize this section, it can be said that the lowest quantum state of neutrons in the gravitational field was clearly identified using the "flow-through" mode, which measures the neutron flux as a function of an absorber/scatterer height. This observation itself already makes many interesting applications possible. Higher quantum states could also be resolved. However, such a measurement is much more complicated because the energy (or height) resolution of the present method is limited by one main factor: the finite sharpness of the dependence on height of neutron tunneling through the gravitational barrier between the classically allowed height and the scatterer height.

4 Studies of the Neutron Quantum States in "Differential" Flow-Through Mode

In order to resolve higher quantum states clearly and measure their parameters accurately, we must adopt other methods, such as for example, the "differential" method, which uses position-sensitive neutron detectors with a very high spatial resolution, which were developed specifically for this particular task [21].

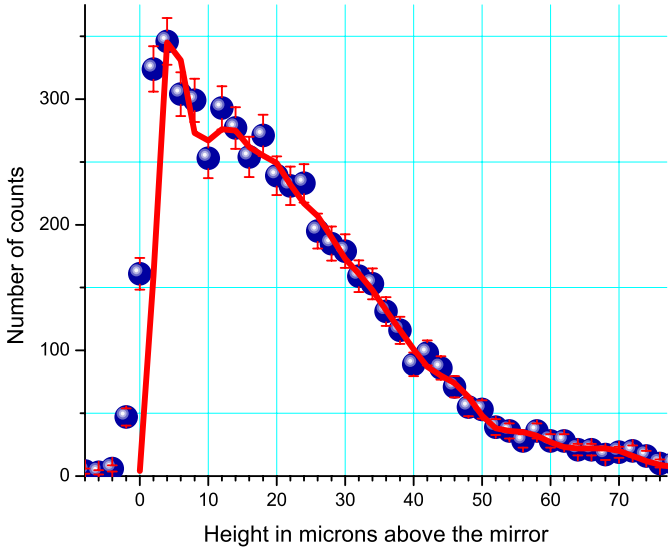

Fig. 5. The results of the measurement of the neutron density above a mirror in the Earth's gravitational field are obtained using a high-resolution plastic nuclear-track detector with uranium coating. The horizontal axis corresponds to a height above the mirror in microns. The vertical axis gives the number of events in an interval of heights. The solid line shows the theoretical expectation under the assumption that the spatial resolution is infinitely high. Calculated populations of the quantum states correspond to those measured by means of two scatterers using the method shown in Fig. 6.

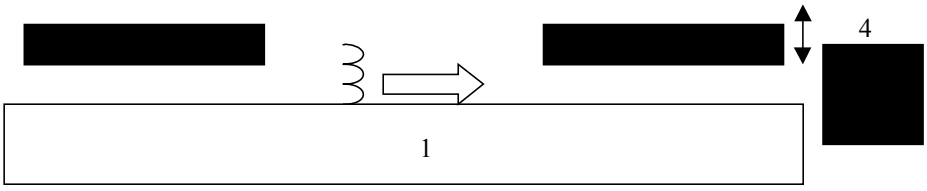

Fig. 6. A scheme of the experiment with a long bottom mirror (1, shown as the open box) and with two scatterers (2, 3, shown as the black boxes). The first scatterer (2, on the left) shapes the neutron spectrum. It is installed at the constant height of 42 μm. The second scatterer (3, on the right) analyses the resulting neutron spectrum. Its height is varied. The detector (4), shown as the black box, measures the total neutron flux at the exit of the slit between the mirror and the analyzing scatterer. The distance between the scatterers is equal to 9 cm.

The direct measurement of the spatial density distribution in a standing neutron wave is preferable to its investigation with the aid of a scatterer whose height can be adjusted. The former technique is differential, since it permits the simultaneous measurement of the probability that neutrons reside at all heights of interest. The latter technique is integral, since the information on the probability that neutrons reside at a given height is in fact obtained by the subtraction of the values of neutron fluxes measured for two close values of the scatterer height. Clearly, the differential technique is much more sensitive than the integral one and makes it possible to gain the desired statistical accuracy much faster. This is of prime importance considering the extremely low counting rate in this experiment, even with the use of the highest UCN flux available today. Furthermore, the scatterer employed in the integral technique inevitably distorts the measured quantum states by deforming their eigen-functions and shifting their energy values. The finite accuracy of taking these distortions into account results in systematic errors and ultimately limits the attainable accuracy of the measurement of the quantum state parameters. For these and other reasons, the use of a position-sensitive detector to directly measure the probability of neutron residence above the mirror is highly attractive. However, until now there were no neutron detectors with the spatial resolution of ~1 μm needed for this experiment. We therefore had to develop such a detector and measuring technique. The result was a plastic track nuclear detector (CR39) with a thin uranium coating ($^{235}UF_4$), described in ref. [21]. The tracks created by the entry into the plastic detector of a daughter nucleus produced by the neutron-induced fission of a ^{235}U nucleus were increased to ~1 μm in diameter by means of chemical development in an alkaline solution. The developed detector was scanned with an optical microscope over a length of several centimeters with an accuracy of ~1 μm. The sensitive ^{235}U layer is thin enough (<1 μm) for the coordinates of neutron entry into the uranium layer to almost coincide with the coordinates of daughter nucleus entry into the plastic. On the other hand, the sensitive layer is thick enough to ensure high UCN detection efficiency (~30 %). The measuring technique and the preliminary analysis of the results are described in ref. [15].

The feasibility of this technique was demonstrated in the second experiment and the results are presented in Fig. 5 [15]. This is the first direct measurement of the neutron density above the mirror with a spatial resolution of 1-2 μm. The theoretical curve presented in Fig. 5 is calculated with known neutron wave functions and with the quantum level populations and the zero height above the mirror as free parameters. The spatial detector resolution is assumed to be perfect. A comparison of the experimental data with the theoretical prediction suggests that: firstly, the measured presence probability for neutrons above the mirror on the whole domain of Δz corresponds closely to the theoretical prediction; secondly, the spatial detector resolution can be estimated, for instance, using the steepest portion of the dependence near the zero height, which is equal to ~1.5 μm; finally, even a relatively small neutron density variation of ~10%, which is to be expected for the mixture of several quantum states employed in this experiment, can be measured using this technique. It should be noted that this measurement was performed in the special geometry of the mirror and the scaterrers shown in Fig.6. A long bottom mirror (1) was used with two scatterers (2) and (3). The first scatterer gives the neutron spectrum the desirable shape and is installed at the constant height of 42 μm. The second one analyses the resulting neutron spectrum; its height is varied. The detector (4), shown as the black box, measures the total neutron flux at the exit of the slit between the mirror and the analyzing scatterer. The distance between the scatterers is equal to 9 cm.

However, the measurement presented in Fig. 5 is merely a test of the detector for spatial resolution and is not optimized for studying the neutron quantum states in this system. In ref. [20], the measurement with the position-sensitive detector was analyzed from the standpoint of its optimization for the identification of neutron quantum states. Fig. 1 depicts the probability $\psi_n^2(z)$ of neutron detection at a height z above the mirror surface for 4 pure quantum states. Clearly, every dependence $\psi_n^2(z)$ has n maxima and $n-1$ minima between them with zero values at the minima, which is characteristic of any standing wave. An ideal experiment would consist of the extraction of one or several pure quantum states higher than the first one ($n>1$) and the direct measurement of neutron detection probability against the height above the mirror with the aid of a position-sensitive detector with a spatial resolution of ~1 μm.

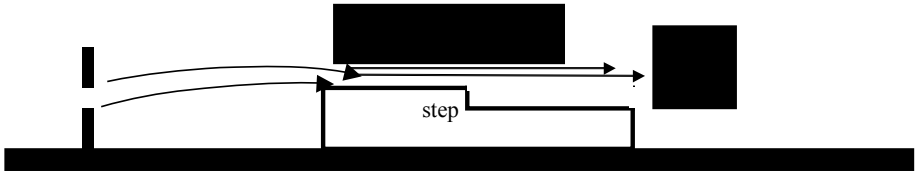

Fig. 7. A scheme of the experiment with a small negative step on the lower mirror, which allows the transition of neutrons to higher quantum states (to the region to the right of the step).

Let us consider a possible method for carrying out such an experiment. One or two lower quantum states can be selected with a scatterer by the conventional method adopted in all our previous experiments, which showed that the spectrometer resolution is sufficient for this. The method for transferring neutrons from the lower quantum states to the higher quantum states was considered in ref. [22]. It involves the fabrication of a small negative step on the lower mirror, as shown in Fig. 7. Neutrons are in quantum states both to the left of the step and to the right of the step. However, the corresponding wave functions have shifted relative to each other by the step height Δz_{step}. By passing through the step, neutrons are redistributed from the n^{th} quantum state prior to the step $\psi_{\text{before}}(z)=\psi_n(z+\Delta z_{\text{step}})$ over the quantum state $\psi_{\text{after}}(z)=\psi_n(z)$ after the step with some probabilities $\beta_{nk}^2(\Delta z_{\text{step}})$. In this case, the step can be treated as an infinitely fast perturbation and therefore the transition matrix element $\beta_{nk}(\Delta z_{\text{step}})$ is:

$$\beta_{nk}(\Delta z_{\text{step}})=\int_0^\infty \psi_n(z+\Delta z_{\text{step}})\psi_k(z)dz\,. \tag{4.1}$$

Fig. 8 shows the calculated probability $\beta_{1k}^2(\Delta z_{\text{step}})$ of transition from the 1st quantum state, prior to passing through the step, to the 1st, 2nd, 3rd and 4th quantum states after passing through the step.

When the negative step is large enough, for instance is equal to (–15 μm), the probability β_{11}^2 to detect neutrons in the lowest quantum state after passing through the step is extremely small. The similar probability β_{n1}^2 for neutron transitions from higher initial quantum states is also low. Any overlap integral β_{n1}^2 for $\Delta z_{\text{step}} = -15\ \mu\text{m}$ is small, since the spatial dimension of the neutron wave function in the lowest quantum state $\psi_1(z)$ is smaller than 15 μm.

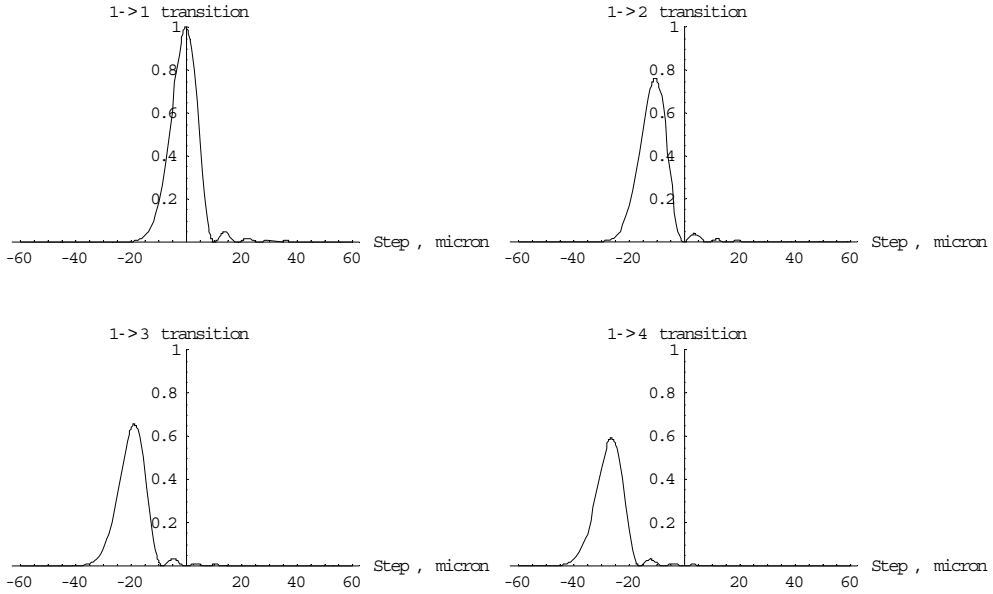

Fig. 8. Probability of neutron transition from the 1st quantum state, prior to transit through the step, to the 1st, 2nd, 3rd and 4th quantum states on transit through the step as a function of the step height Δz_{step}.

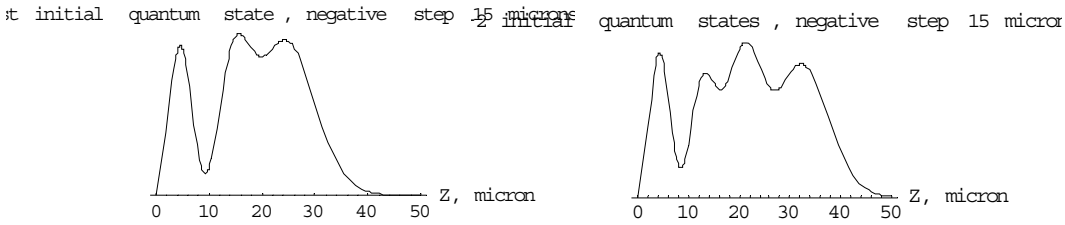

Fig. 9. Probability of neutron residence versus height above the mirror on neutron transit through a negative 15-μm step for two cases: one and two lowest quantum states prior to the passage through the step.

Fig. 9 shows the probability of neutron detection above the mirror depending on the height after the neutron passes through the negative 15-μm step. The probability is plotted in two cases: for one and two quantum states prior to passing through the step. It is evident that the expected spatial variation of neutron density is clearly defined and can be measured. The

reason for such a strong neutron density variation in the case of the elimination of the lowest quantum state is simple: we can see from Fig. 1 that only the lowest quantum state has a peak near 10 μm. The remaining low-lying quantum states possess a minimum at this height. Therefore, several lower quantum states ($n > 1$) are "coherently" combined: the probability of neutron detection at a height of ~10 μm is systematically much lower than for neighboring heights.

This idea was demonstrated in the last experiment performed in the summer of 2004 [23]. A neutron beam with a horizontal velocity component of ~5 m/sec and a vertical velocity component of 1–2 cm/sec, which corresponds to the energy of the lowest neutron quantum state in the gravitational field above a mirror, is selected using a bottom mirror (1) and a scatterer/absorber (3) positioned above it at a height of ~20 μm. A second mirror (2) is installed 21 μm lower than the first mirror (1). The precision of the optical components' adjustment and the neutron detection resolution are equal to ~1 μm.

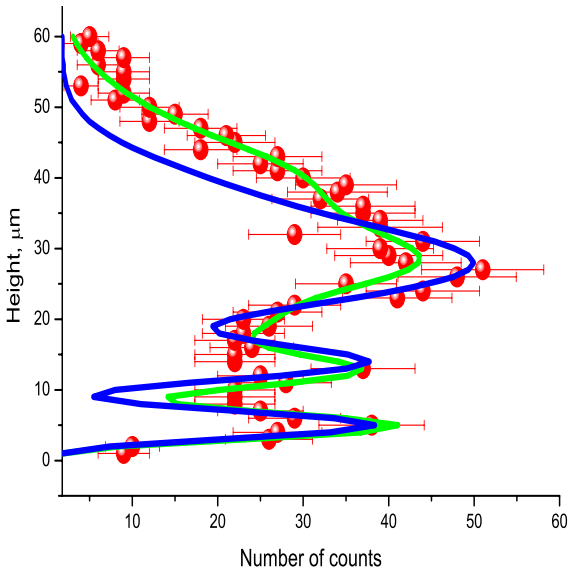

Fig. 10. The neutron density distribution in the gravitational field is measured using position-sensitive detectors of extra-high spatial resolution. The circles indicate experimental results. The solid curve corresponds to the theoretical expectation under the assumption of an ideally efficient scatterer able to select a single quantum state above the mirror (1) and no parasitic transitions between the quantum states above the mirror (2). The dotted curve corresponds to the more realistic fit using precise wave-functions and free values for the quantum states populations (for simplicity, the intereference terms between different levels are neglected). The detector background is constant in the range from –3 mm to +3 mm below and above the presented part of the detector.

Typical results of a few days' detector exposure in such an experiment are presented in Fig. 10. Even if the analysis of these data has not yet been completed and the fine details of the quantum states can not be extracted, we can see clearly that the experimental approach developed here allows us to obtain a very pronounced variation of the wave function and can thus be considered as very promising.

The characteristic behavior of the neutron wave functions in the quantum states in the gravitational field above the mirror, as well as the successful initial testing of the position-sensitive detector with a uranium coating, suggest that it will be possible to identify neutron quantum states by directly measuring the neutron detection probability above a mirror using the position-sensitive detector. It should be noted that this detector could be also used to measure the velocity distribution in quantum states. To do so, we need simply to shift the detector a few centimeters downstream to the bottom mirror edge: the spatial spread of the picture thus obtained will not be sensitive to the initial position of the neutron above the mirror but to its velocity.

Thus, the two techniques considered and the available fluxes of UCN are already sufficient for a broad range of applications. Let us analyze them briefly, before considering further developments of this experiment, related to resonance transitions between different quantum states and thus to a much more precise measurement of the parameters of these quantum states.

5 Use of Neutron Quantum States in Different Domains of Physics

As we have already mentioned in section 3, further development [18] of the theoretical description of this experiment and experimental efforts related to improving the accuracy of the absolute positioning of the scatterer [19, 20] could allow us to achieve close to a few percent accuracy in the determination of quantum state parameters. It should also be noted that the direct measurement of the spectral variation of neutron density above mirror in the quantum states seem to be quite promising. For this reason we are rather confident that, even at this early stage we can already obtain some interesting physical results using this method.

For instance, as shown in ref. [24] and presented here in section 5.1, a competitive upper limit for short-range fundamental forces was obtained simply from the very fact that the gravitationally bound quantum states exist. Moreover, if any additional short-range interaction were to exist (of whatever nature: new hypothetical particles, supplementary spatial dimensions, etc.), this would change the parameters of the neutron quantum states. Therefore, the precise measurement of these parameters gives an upper limit for unknown interactions.

This experiment can also be used to search for the axion – a hypothetical particle which strongly violates CP invariance; the characteristic distance for this interaction is comparable to the characteristic length of our problem z_0. This is discussed in section 5.2 and can be considered within the more general context of studies of spin-gravity interaction.

This method could be used for studies related to the foundations of quantum mechanics, such as for instance, the quantum-mechanical localization (also known as quantum revivals, see section 5.3) [25], or various extensions of quantum mechanics [26, 27] (see section 5.4). One should note here that the present method provides two unique opportunities: on the one hand, it provides a rare combination of quantum states and gravitation that is favorable for testing possible extensions of quantum mechanics; on the other hand, UCN can be reflected from the surface up to $\sim 10^5$ times without loss, i.e. much more than for optical phenomena, which means that any kind of localization can be better studied using UCN. Finally, as

presented in section 5.5, this method could be useful for such problems of high long-term interest as the loss of quantum coherence in the systems with gravitational interaction (see, for instance, refs. [28, 29]).

5.1 Search for Non-newtonian Gravity

According to the predictions of unified gauge theories, super-symmetry, super-gravity and string theory, there exist a number of light and massless particles [30]. An exchange of such particles between two bodies gives rise to an additional force. Additional fundamental forces at short distances have been intensively studied, in particular over the past few years in the light of the hypothesis about "large" supplementary spatial dimensions proposed by Antoniadis, Arkami-Hamed, Dimopoulos and Dvali [31] and based on earlier ideas presented in [32–35]. A review of theoretical works and recent experimental results can be found in [36–40]. This hypothesis could be verified using neutrons because the absence of an electric charge makes it possible to strongly suppress the false electromagnetic effects [41]. It was noticed in [42] that the measurement of the neutron quantum states in the earth's gravitational field is sensitive to such extra forces in the sub-micrometer range. In the case of $n = 3$ extra dimensions, the characteristic range lies just within the nanometre domain [31, 41] which is accessible in this experiment. The first attempt to establish a model-dependent boundary in the range 1–10 μm was presented in [40].

An effective gravitational interaction in the presence of an additional Yukawa-type force is conventionally parameterized as:

$$V_{\text{eff}}(r) = G\frac{m_1 m_2}{r}\left(1+\alpha_G e^{-r/\lambda}\right) \tag{5.1}$$

Here, G is the Newtonian gravitational constant, m_1 and m_2 are interacting masses, r their relative distance, α_G and λ are the strength and characteristic range of this hypothetical interaction.

The dependence of neutron flux on the slit size is sensitive to the presence of quantum states of neutrons in the potential well formed by the earth's gravitational field and the mirror. In particular, the neutron flux was found to be equal to zero within the experimental accuracy if the slit size Δz was smaller than the characteristic spatial size (a quasi-classical turning point height) of the lowest quantum state of ~15 μm in this potential well. The neutron flux at the slit size $\Delta z < 10\ \mu\text{m}$ in the second experiment [15] was lower by at least a factor of 200 than that for the lowest quantum state ($\Delta z \approx 20\ \mu\text{m}$).

If an additional short-range force of sufficiently high strength were to act between the neutrons and the mirror then it would modify the quantum states parameters: an attractive force would "compress" the wave functions towards the mirror, while a repulsive force would shift them up. In this experiment, no deviation from the expected values was observed within the experimental accuracy. This accuracy is defined by the uncertainty in the slit size, which can be conservatively estimated as ~30% for the lowest quantum state [15].

As we mentioned in section 2, the motion of neutrons in this system over the vertical axis z could be considered, in a first, relatively good approximation, as a one-dimensional problem for which the mirror provides an infinitely high potential. The interaction between neutrons and the Earth is described by the first term in eq. (5.1) and can be approximated by the usual linear potential $(r = R + z)$:

$$V(z) = mgz \tag{5.2}$$

with $g = GMm / R^2$, R being the Earth's radius, M its mass.

The second term in eq. (5.1) introduces an additional interaction. Due to the short range of this interaction, its main contribution is provided by the interaction of neutrons with a thin surface layer of the mirror and the scatterer.

Let us first estimate the interaction of neutrons with the mirror due to this additional term if this interaction is attractive. If the mirror's density is constant and equal to ρ_{m}, then an additional potential of the interaction between the neutrons and the mirror, in the limit of small λ, is given by [24]:

$$V'(z) = -U_0 e^{-z/\lambda} \tag{5.3}$$

with $U_0 = 2\pi G \alpha_G m \rho_{\mathrm{m}} \lambda^2$.

The simplest upper limit on the strength of an additional interaction follows from the condition that this additional interaction does not itself create any bound state. It is known [7] that for an exponential attractive ($U_0 > 0$) potential (5.3) this means that

$$\frac{U_0 m \lambda^2}{\hbar^2} < 0.72 \cdot \tag{5.4}$$

This condition gives a boundary for an additional potential strength:

$$\alpha_G = 0.72 \frac{2}{\pi} \frac{\rho}{\rho_{\mathrm{m}}} \frac{\hbar}{mg\lambda^2} \frac{\hbar}{m\lambda} \frac{R}{\lambda} \tag{5.5}$$

ρ being the Earth's average density. In this experiment, both densities are close to each other $\rho \approx \rho_{\mathrm{m}}$, therefore their ratio ρ / ρ_{m} is close to 1. However, a suitable choice of mirror material (coating) would easily allow us to gain a factor of 3–5 in the sensitivity in future experiments. We obtain the following numerical boundary:

$$\alpha_G = 1 \times 10^{15} \left(\frac{1\ \mu\mathrm{m}}{\lambda} \right)^4 . \tag{5.6}$$

Here, 1 μm is chosen as a natural scale for this experiment. This limit is presented in Fig. 11 in comparison with the limits from the Casimir-like and van der Waals force measurement

experiments [38], as well as from experiments on protonium atoms. An additional force between a nucleus and an antiproton would change the spectrum of such an atom. The most precise measurement of the energy spectrum of antiprotonic atoms was done for $^3He^+$ and $^4He^+$ atoms by the ASAKUSA collaboration at the antiproton decelerator at CERN [44]. No deviation was found from the values expected within the QED calculations [43]. An 1σ upper limit on $|\alpha_G|$ from this experiment was established in [24]:

$$|\alpha_G| = 1.3\times10^{28}. \tag{5.7}$$

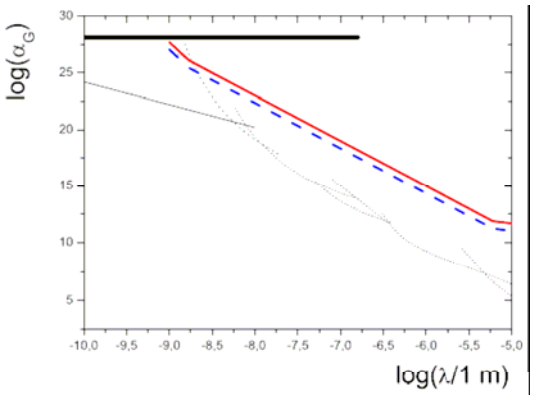

Fig. 11. The constraints on α_G following from this experiment [12, 13] (the solid line) in comparison with that from the measurement of the Casimir and the van derWaals forces [35] (the short dashed lines). The long dashed line shows a limit which can be easily obtained by an improvement of this experiment. The solid horizontal line represents the limit established from the atomic experiment [41]. Dash-dotted line shows the limit which would be obtained if one equals the strength of this additional hypothetical interaction to the value of effective Fermi potential for Pb [43].

It is necessary to note that, in the realistic case, one has to establish a condition of non-existence of an additional bound state for the sum of (5.2) and (5.3) but not for the interaction (5.3) alone. The presence of the linear potential modifies slightly the critical value in (5.4). For instance, for $\lambda = 1\ \mu$m it is approximately equal to 1.0 and for $\lambda = 0.1\ \mu$m it is equal to 0.74. For smaller λ, this value tends to 0.72. It is possible to explain qualitatively why the strength of an additional interaction should be higher in the presence of the *mgz*-potential than without it. When a bound state has just appeared, then its wave function is extremely spread. If a supplementary "external" confining potential is added, it does not allow the wave function to be spread and thus a stronger potential is needed to create a bound state.

The range of presented λ is 1 nm–10 μm. A deviation from a straight line in the solid curve at 1 nm is due to the finite range of increase of the mirror effective nuclear potential (impurities on the surface and its roughness). The same effect at $\lambda \approx 10\ \mu$m is due to "interference" between the potentials (5.2) and (5.3).

Unfortunately, this experiment does not allow us to establish a competitive limit for a repulsive interaction. In this case, there could be no "additional" bound state. Here, instead of the condition of "non-existence" of a bound state, one could consider the critical slit size for

which the first bound state appears in this system. Such an approach would be model-dependent due to uncertainties in the description of the interaction of neutrons with the scatterer. Nevertheless, it is possible to obtain a simple analytical expression for small λ and to show explicitly a difference in the sensitivity of this experiment to an attractive and to a repulsive additional interaction.

$$\alpha_G = \frac{1}{\pi}\frac{\rho}{\rho_{\mathrm{m}}}\frac{\hbar}{mg\lambda^2}\frac{\hbar}{m\lambda}\frac{R}{\lambda}\exp\left(\lambda_0/\lambda\right) \tag{5.8}$$

with $\lambda_0 = \delta E_n / mg$, δE_n being the precision of determination of the *n*-th quantum state energy.

A direct comparison of relation (5.8) to (5.5) shows that the limit (5.8) at small λ is sufficiently less restrictive than the limit for an attractive one (5.5) due to the exponential factor. On the other hand, it would be possible to achieve as strict a limit for a repulsive interaction as for an attractive one, if the mirror was coated with a material with negative Fermi potential.

As a conclusion, let us emphasize that even though this experiment was never designed to search for additional short-range forces it provides the competitive limit (5.5) in the nanometer range. However, it could be easily improved in the same kind of experiment by making some obvious modifications. For instance, one could choose a mirror material (coating) with a higher density. A significant improvement to such a limit would only seem possible by using the "storage" method, which would allow a gain in accuracy of a few orders of magnitude.

A more significant gain in the sensitivity could be achieved in dedicated neutron experiments. Simply as a qualitative illustration of the potential capacities of experiments with neutrons, it can be said that if the strength of this additional hypothetical interaction were equal to the value of effective Fermi potential for Pb [46] this equality would produce the limit presented by the dash-dotted line in Fig. 11.

5.2 Search for the Axion and Spin-Gravity Interaction

Axions are well-known as a possible solution to the strong CP problem as well as an interesting darkmatter candidate [47]. One of the most remarkable predictions associated with the axion is that it yields a parity and time-reversal violating, monopole-dipole coupling between spin and matter [48]. Experimental and astrophysical observations imply that the mass of the axion must lie between 1 μeV and 1 meV, corresponding to a range between 20 cm and 0.2 mm [49]. This range is commonly referred to as the "axion window." An exhastive review of theoretical and experimental activities to search for the axion can be found in [30].

Axions mediate a CP violating monopole-dipole Yukawa-type gravitational interaction potential [48]

$$V(\vec{r}) = \hbar g_p g_s \frac{\vec{\sigma}\cdot\vec{n}}{8\pi mc}\left(\frac{1}{\lambda r}+\frac{1}{r^2}\right)e^{-r/\lambda} \tag{5.9}$$

between spin and matter where $g_p g_s$ is the product of couplings at the scalar and polarized vertices and λ is the range of the force. Here r is the distance between the neutron and the nucleus and $\vec{n}=\vec{r}/r$ a unitary vector.

Untill now, only a few experiments placed upper limits on the product coupling $g_p g_s$ in a system of magnetized media and test masses. Of the experiments covering the axion window, one of them [50] had peak sensitivity near 100 mm (2 μeV axion mass) and another [51] had peak sensitivity near 10 mm (20 μeV axion mass).

Let us make an initial qualitative estimation of the limit of the axion coupling constant which can be established from the existing experiment. The upper limit for which the peak of sensitivity is clearly close 10 μm.

By analogy with the demonstration presented in the previous section where an additional interaction between (5.1) the neutron and the mirror's nuclei created an additional neutron-mirror interaction potential (5.3), in the case of the interaction (5.9), a neutron with a given projection of spin on the vertical (*g*) axis will see an additional potential with the following shape created by the whole mirror:

$$U(z_0) = \frac{g_p g_s}{4\pi}\frac{\pi\hbar\rho_m\lambda}{2mm_A c}e^{-z_0/\lambda}. \tag{5.10}$$

This potential, considered as a perturbation, will produce a positive energy shift ε_0 (in the first order of the perturbation theory) for one of two possible spin projections and a negative energy shift $-\varepsilon_0$. Thus obtained, the energy splitting can be constrained from the experimental data. For instance, we can propose a very rough and robust upper limit if we says that this splitting is smaller than at least half of the energy difference between two gravitational levels:

$$2\varepsilon_0 \le \frac{1}{2}\left(E_2 - E_1\right) \equiv \frac{1}{2}\Delta E \tag{5.11}$$

Therefore the limit of the axion coupling constant will be given by

$$\frac{g_p g_s}{\hbar c} = \frac{2\Delta E mm_A}{\hbar^2\rho_m\lambda} \tag{5.12}$$

(here the exponential function is replaced by 1, because the size of the wave function is of the order of ten micrometers whereas the range of the interaction, for the axion window, is higher than 100 microns).

To obtain a naive estimation for $\lambda = 1$ mm, we can suppose that $m_A = 20m$, $\Delta E = 1$ peV (i.e. the energy difference between two gravitational levels), $\rho_m = 4000$ kg/m^3:

$$\frac{g_p g_s}{\hbar c} = 4 \cdot 10^{-16}. \tag{5.13}$$

This limit is at least a few orders of magnitude better than the limit obtained in the experiments [50, 51].

In principle, a very competitive constraint could be obtained using the present flow-through method for spin-dependent short-range forces in a dedicated experiment with polarized neutrons. By alternating the neutron spin in such an experiment an accuracy of $\sim 10^{-3} - 10^{-4}$ could easily be achieve (instead of 1 considered in the estimation given here). The main simplification in the case of spin-dependent forces is the relative nature of the measurement, because the neutron spin can be easily flipped with a high accuracy. In contrast to that, spin-independent forces can not be "switched off". We would therefore need an absolute measurement in this case.

Let us emphasize that this discussion can be seen as a part of the wider search for spin-gravity interaction. The idea that a nuclear particle may possess a gravitoelectric dipole moment was proposed about forty years ago by Kobsarev and Okun [52] and by Leitner and Okubo [53]. A brief review of experimental and theoretical activity on this question can be found in [54]. Here we would like to emphasize that this problem has been discussed at length in a number of recent articles, with arguments for [52] and against [56] this kind of term (5.10) in the interaction of fermions with an external gravitational field, and that the inrtoduction of polarized neutrons into our experiment does not represent a difficult experimental challenge.

5.3 Quantum Revivals

The application of this experiment to quantum mechanical localization (also known as quantum revivals) was considered in detail in a recent review article by Robinett [25]. Let us remind the reader of the main ideas presented there and the feasibility of such a measurement in our experimental setup.

Quantum revivals are characterized by initially localized quantum states which have a short-term, quasi-classical time evolution, which then can spread significantly over several orbits, only to reform later in the form of a quantum revival in which the spreading reverses itself, the wave packet relocalizes, and the semi-classical periodicity is once again evident.

The study of the time-development of wave packet solutions of the Schrödinger equation often makes use of the concept of the overlap $\langle \psi_t | \psi_0 \rangle$ of the time-dependent quantum state $|\psi_t\rangle$ with the initial state $|\psi_0\rangle$. This overlap is most often referred to as the autocorrelation function.

For one-dimensional bound state systems, where a wave packet is expanded in terms of energy eigenfunctions $\psi_n(x)$ with quantized energy eigenvalues E_n in the form

$$\psi(x,t) = \sum_{n=1}^{\infty} a_n \psi_n(x) e^{-iE_n t/\hbar} \tag{5.14}$$

with

$$a_n = \int_{-\infty}^{\infty} \psi_n^*(x)\psi(x,t)dx \tag{5.15}$$

the autocorrelation function can be written as:

$$A(t) = \sum_{n=1}^{\infty} \left|a_n\right|^2 e^{iE_n t/\hbar} \tag{5.16}$$

and the evaluation of $A(t)$ in this form for initially highly localized wave packets will be investigated experimentally.

If a localized wave packet is excited with an energy spectrum which is tightly spread around a large central value of the quantum number n_0 so that $n_0 \gg \Delta n \gg 1$, it is possible to expand the individual energy eigenvalues, $E_n \equiv E(n)$, about this value, giving

$$E(n) \approx E(n_0) + E'(n_0)(n-n_0) + \frac{E''(n_0)}{2!}(n-n_0)^2 + \frac{E'''(n_0)}{3!}(n-n_0)^2 + \ldots \tag{5.17}$$

This gives the time-dependence of each individual quantum eigenstate through the factors:

$$e^{iE_n t/\hbar} = e^{i\omega_0 t} \cdot e^{i2\pi(n-n_0)/T_{cl}} \cdot e^{i2\pi(n-n_0)^2/T_{rev}} \cdot e^{i2\pi(n-n_0)^3/T_{super}}, \tag{5.18}$$

where each term in the expansion (after the first which is an unimportant overall phase not observable experimentally) defines an important characteristic time scale, via:

$$T_{cl} = \frac{2\pi\hbar}{\left|E'(n_0)\right|},\ T_{rev} = \frac{4\pi\hbar}{\left|E''(n_0)\right|} \text{ and } T_{super} = \frac{12\pi\hbar}{\left|E'''(n_0)\right|}. \tag{5.19}$$

The second term in the expansion is associated with the classical period of motion in the bound state. It can also be shown that the wave packet near the revival time T_{rev} returns to something like its initial form, exhibiting the classical periodicity. In the special case when T_{rev}/T_{cl} is an integer, the revival occurs exactly in phase with the original time-development, and is exact (in that $\left|A(t)\right|$ returns to exactly unity). For some realistic systems, with higher order terms in the expansion in Eq. (5.17), the superrevival time, T_{super} also becomes very important.

To obtain the order of magnitude of the different characteristic times introduced previously, one can consider a neutron in the second state. For this state, the value of the classical turning point (2.11) is equal to $z_2 = 24\ \mu\text{m}$. The classical periodicity of the system is given by

$$T_{cl} = 2\sqrt{\frac{2z_2}{g}} \approx 4.4\ \text{ms}. \tag{5.20}$$

The revival time appears to be equal to

$$T_{rev} = \frac{16mz_0^2}{\pi\hbar} \approx 46\ \text{ms}. \tag{5.21}$$

With the neutrons of 5 m/s velocity, a 25 cm long mirror is needed to observe this revival phenomenon.

All the methodical developements for this kind of experiments are already available: the position-sensitive detector discussed in section 3 can provide the spatial resolution of 1 μm, the absorber/scatterer and a suitable mirror geometry (see sections 2 and 3) make it possible to chose the necessary number of quantum states, and the phase of the wave function can be fixed by a special collimator at the entry to the system.

5.4 Search for a Logarithmic Term in the Schrödinger Equation

As discussed in refs. [26, 27], an extension of quantum mechanics with an additional logarithmic term in the Schrödinger equation assumes quasi-elastic scattering of UCN at the surface, with extremely small, but nevertheless measurable, energy changes. Such spectral measurements of high resolution with UCN were themselves methodologically challenging. They were also motivated by a long-standing anomaly in the storage of UCN in traps [57]. These experiments [58, 59] allowed the authors to constrain such quasi-elasticity at ~10^{-11} eV per collision, under the assumption of a "random walk" in phase space at each neutron collision with the wall: a non-zero result at this level was reported in ref. [58] at the limit of experimental sensitivity, but was not confirmed later in ref. [59], measured in the same setup with slightly better statistical sensitivity but with worse energy resolution.

A significant increase in the accuracy of neutron gravitational spectrometry using the high-resolution position-sensitive neutron detectors presented here allows us to improve many times over the upper limit for the probability and for the minimum energy transfer values for the quasi-elastic scattering of UCN at the surface [60]. Moreover, we can now consider energy changes at a single reflection, rather then having to follow the integral effects of many collisions, as in refs. [58, 59]. In addition to this, the present limit concerns one specific component of the neutron velocity along the vertical axis before reflection and after it. Also any deviation from conventional quantum mechanics can be verified in a more direct way with the quantum limit used here for the minimum possible initial energy, or velocity.

Such constraints, however, present a broader interest and could be considered in a more general model-independent way: how precisely do we know that UCN conserve their energy at wall reflections or during UCN storage in material traps?

Let us remind the reader of the details of the experimental set up used in the last run. A neutron beam with a horizontal velocity component of ~5 m/sec and a vertical velocity component of 1-2 cm/sec, which corresponds to the energy of the lowest neutron quantum state in the gravitational field above a mirror, is selected using a bottom mirror (1) and a scatterer/absorber (3) positioned above it at a height of ~20 μm. A second mirror (2) is installed 21 μm lower than the first mirror (1). If the UCN bounce elastically on the mirror (2) surface in the zone between the scatterer's (3) exit edge and the position-sensitive detector (4), the measured spatial variation of the neutron density as a function of height would correspond to that shaped by the mirrors (1,2) and the scatterer (3) in the zone upstream of the scatterer's (3) exit edge. If they do not, then the excess number of neutrons observed in the higher position would be attributed to their quasi-elastic reflection from the mirror (2) surface. The experimental setup is designed in such a way that any known parasitic effects (vibration of the mirrors and the scatterer, residual magnetic field gradients, quasi-specular reflections of UCN from mirrors or at residual dust particles) should be small enough not to cause a significant change in the spectrum of vertical neutron velocities (see refs. [8-9, 19-22]).

We will not discuss the possible microscopic mechanisms of quasi-elastic reflections of UCN at surfaces; we shall simply consider this problem in phenomenological terms. A simple conservative upper limit for the quasi-elastic scattering/heating probability (versus average energy transfer) following UCN reflection from the lower polished glass mirror could be calculated, assuming an ideal scatterer able to select a single quantum state above the mirror (1) in Fig. 7. Populations of all quantum states above the mirror (2) can be precisely calculated in this case [22]. They provide the neutron density distribution, presented by the solid curve in Fig. 10. We know in fact that a few neutrons at higher quantum states should survive [15] producing a density distribution close to one presented by the dotted curve in Fig. 10. However, we do not attempt to take such neutrons into account and intentionally sacrifice the sensitivity of the present limit in favor of maximum reliability and transparency. Such an estimation could be further improved with the present experimental data using a more sophisticated theoretical analysis based on ref. [15]. It would however be slightly model-dependent in such a case. For the simplified approach chosen, the solid line in Fig. 10 is considered as "background" for the measurement of quasi-elasticity and any additional events above this line would be supposed to be due to quasi-elastic scattering. Fig. 12 illustrates the results of the treatment of the experimental data presented in Fig. 10.

The straightforward calculation of such a constraint provides the solid curve in Fig. 12 under the following assumptions: 1) all additional events higher than the solid curve in Fig. 10 are attributable to quasi-elastic scattering/heating; 2) the energy is assumed to change in one step (due to the low probability of such an event); 3) we take the number of quasi-classical collisions in such a system [15].

The rather sharp decrease with height of the neutron density on a characteristic scale of a few microns simplifies considerably the present calculation. For large enough ΔE values, any excess counts above the constant background level $\Delta N_{\mathrm{bg}} / \Delta h$ in the height range $h > 60\ \mu\mathrm{m}$ are attributed to quasi-elastic scattering/heating. Quasi-elastically scattered

neutrons could be observed at any height between zero and $(E_0 + \Delta E)/mg$, where E_0 is the initial energy of vertical motion and ΔE is the energy gain. If $\Delta E \gg E_0$, the total number of background events is approximately equal to $\frac{\Delta N_{bg}}{\Delta h}\frac{\Delta E}{mg}$, neglecting the initial spectral line width $h < 60\ \mu$m. At 3σ confidence level, we would observe an excess N_{qel} of events at $h > 60\ \mu$m, if it is equal to:

$$N_{qel} = 3\sqrt{\frac{\Delta N_{bg}}{\Delta h}\frac{\Delta E}{mg}}. \tag{5.22}$$

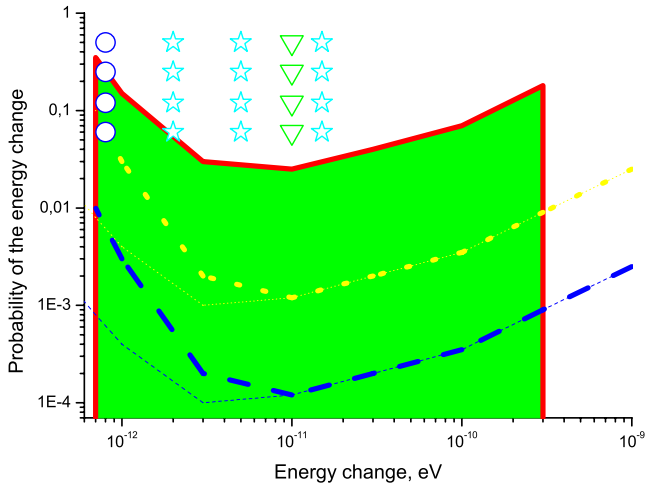

Fig. 12. The solid curve corresponds to constraints for quasi-elastic scattering of UCN at a flat glass surface: the total probability of such a scattering per one quasi-classical bounce versus average energy transfer at "3σ" confidence level. The dotted curve shows the possible improvement of such constraints in the flow-through measuring mode. The dashed curve indicates a further increase in sensitivity in the storage measuring mode. The circles correspond to theoretical predictions for the present experiment in accordance with refs. [14-15, 17]. The stars indicate analogous predictions for measurements with the experimental setup [8-9, 19-22] inclined to various angles. The triangles show the value of the energy change expected in refs. [14-15, 17] (for a higher initial neutron velocity than that in the present experiment). The thin dotted and dashed curves indicate schematically the constraints if the initial spectral shape line were to be taken into account.

With the horizontal velocity component v_{hor} and the mirror length L between the scatterer's exit edge and the detector (see Fig. 7), the total number N_{qel} of quasi-classical bounces is:

$$N_{bounces} = \frac{L}{\frac{2}{g}\sqrt{\frac{2E_0}{m}}v_{hor}}. \tag{5.23}$$

Thus, with the total number N_0 of neutrons in the initial spectral line, we would be able to observe quasi-elastic scattering at 3σ confidence level if its probability $P_{\text{qel}}(\Delta E)$ is equal to:

$$P_{\text{qel}}(\Delta E) = \frac{N_{\text{qel}}}{N_0 \cdot N_{\text{bounces}}} = \frac{3}{N_0 L}\sqrt{\frac{\Delta N_{\text{bg}}}{\Delta h}\frac{\Delta E}{mg}}\frac{2}{g}\sqrt{\frac{2E_0}{m}}v_{\text{hor}} \tag{5.24}$$

As is evident from eq. (5.24), $P_{\text{qel}}(\Delta E)$ increases as $\sqrt{\Delta E}$, thus decreasing the sensitivity of the present constraint at large energy changes. The sensitivity is also lower at energy changes smaller than the initial spectral line width of ~60 μm (here the constraint is estimated numerically). Therefore the best sensitivity is achieved at the energy change comparable to one or few initial spectral line widths, as shown in Fig. 12.

The constraint presented shows the high degree of elasticity of neutron reflections in the range $\Delta E \sim 10^{-12} - 3\cdot 10^{-10}$ eV ΔE; this is important for the further development of precision neutron spectrometry experiments. Further improvements in the sensitivity of such constraints by an order of magnitude are feasible in the flow-through measuring mode, by improved shielding of the neutron detectors (a factor $\sqrt{\frac{\Delta N_{\text{bg}}}{\Delta h}}$ in eq. (5.24)), by increasing the length of the bottom mirror (a factor $1/L$ in eq. (5.24)), by further increasing the scatterer efficiency, and by using a narrower initial neutron spectrum (a factor $\sqrt{E_0}$ in eq. (5.24)). On the other hand, a broader initial spectrum could allow us to increase the factor N in eq. (5.24) and therefore to improve the sensitivity at higher ΔE values (sacrificing the sensitivity at lower ΔE values).

An almost order-of-magnitude gain in the minimum measurable energy change could be achieved by providing a proper theoretical account (in accordance with ref. [15], for instance) of the spectrum-shaping properties of the scatterer, or by a differential measurement of the vertical spectrum evolution using bottom mirrors of different lengths. Possible improvements in the flow-through mode are illustrated by the dotted curve in Fig. 12. One should note that any jumps in energy by a value significantly lower than 1 peV would clearly contradict to the observation of quantum states of neutrons in the gravitational field [12–15, 21–23] and therefore they are not analyzed in the present article. The minimum energy increase considered corresponds to the energy difference between neighboring quantum states in the gravitational field.

A much higher increase in sensitivity could be achieved in the storage measuring mode with the long storage of UCN at specular trajectories in a closed trap (the dashed curve in Fig. 12 or better).

As an example of a possible application of the present constraint, let us compare it to the theoretical prediction in accordance with refs. [58,59]. This model assumes the replacement of "continuous interaction" of UCN with a gravitational field by a sequence of "collisions with the field". The time interval $\delta\tau$ between the "collisions" is defined as the time during which the mass "does not know that there is an interaction" since the kinetic energy change δE (by falling) is too small to be resolved. From the uncertainty principle:

$$\delta\tau \cdot \delta E \approx \frac{\hbar}{2}, \text{ or } \delta E \approx \sqrt{\frac{\hbar m g v_{\text{vert}}}{2}} = \sqrt{33 v_{\text{vert}}} \text{ (peV)} \tag{5.25}$$

where v_{vert} is in m/s.

For the vertical velocity component $v_{\text{vert}} \approx 2.5$ cm/s in our present experiment, the expected energy change is $\delta E \approx 8 \cdot 10^{-13}$ eV (shown as the circle in Fig. 12). The "100%" probability of quasi-elastic scattering is slightly higher than the 3σ experimental constraint (the solid line in Fig. 12). However, considering the expected probability value of ~10% and low experimental sensitivity at small ΔE values, one needs to further improve the sensitivity of the present constraint.

On the other hand, a slight modification of the experimental setup would allow us to verify clearly the considered hypothesis. Namely, the whole apparatus should be turned by a significant angle relative to the direction of the gravitational field. In this case, the vertical velocity component is comparable to the longitudinal velocity of 5–10 m/s. The transversal velocity component (relative to the bottom mirror) is very small, just equal to the one in the experiment [12–15, 21–23]. All sensitivity estimations for quasi-elastic scattering/heating are analogous to those given above (see Fig. 12). However, the theoretically predicted effect could be as high as ~10^{-11} eV (depending on the inclination angle) – just in the range of the best sensitivity of the present constraint: the stars in Fig. 12. In order to measure a hypothetical cooling of UCN at their quasi-elastic reflections, we must first of all select a higher quantum state ($n > 1$) and then follow the evolution of the corresponding neutron spectrum. The sensitivity estimations in the energy range $0 < \Delta E < E_0$ would be about as strong as those for the quasi-elastic heating if the experiment was optimized for this purpose. Such measurements would be significantly easier to perform than the measurement of the gravitationally bound quantum states because they do not require such record levels of energy and spatial resolution.

5.5 Search for the Loss of Quantum-Mechanical Coherence

The fundamental loss of quantum coherence because of gravitational interaction is an issue of high long-term scientific interest. As it was pointed out even in the first publication [28], neutron interference experiments could be sensitive to this phenomenon. The quantity defining the sensitivity of such an experiment is the characteristic time of observation of an interference pattern. In the experiment [61] with thermal neutrons this value was about 300 μs (which corresponds to the energy $2 \cdot 10^{-21}$ GeV). In our experimental setup, in the flow-through measuring mode the observation time could be as high as ~60 ms (10^{-23} GeV). A measurement of the localization phenomenon, described in this article, could give a direct estimation of the effect of the fundamental loss of quantum coherence. A much longer observation time would be possible in the storage measuring mode in our experiment. On the other hand, even better constraints for the loss of quantum coherence would be obtained by measuring neutron oscillations between two quantum states due to a small mixing interaction (for instance, a magnetic one) in some analogy to the experiment mentioned in ref. [29].

6 Transitions between the Quantum States

The observation of transitions between the quantum states would allow a qualitatively new step in this research. These transitions can be initiated in various ways and by different forces (strong, electromagnetic, gravitational). In this section we will study, for the first time, different options, giving estimations of probabilities of these transitions.

The mechanical vibration of a mirror would be the simplest way of inducing such transitions. This vibration means a periodical variation of the boundary condition created due to the effective Fermi potential of the bottom mirror (i.e. due to strong forces). In fact, we already observed this kind of transitions induced by nuclear forces, in our last experiment. To suppress neutrons in the ground state, the mirror was assembled in a special way so as to produce a negative step (Fig. 7). This trick can be considered as an infinitely fast change of the Hamiltonian which produces a change in the occupation numbers, i.e. the transitions between the levels.

Another way to produce transitions between the levels is to introduce a varying gradient of magnetic field (i.e. by electromagnetic forces). Until now, all magnetic effects have been considered as parasitic and able to blur the gravitational levels. Considerable efforts were therefore needed to avoid undesirable interaction between the neutron magnetic moment and an external magnetic field. Now that once the existence of the gravitational levels is well-established, a controlled magnetic field can be introduced to manage transitions between the levels. Experimentally, it is easy to produce such a gradient with any form of time-dependence, in particular, perfectly harmonic oscillations.

However, the most interesting way to produce the transitions is by variation of the gravitational field. This could be done, for instance, by the rotation of a massive body close to the experimental set up. This kind of transition is, of course, very difficult to observe. The aim of this study is therefore to evaluate the feasibility of performing this kind of experiment with current and future neutron facilities.

A measurement of transitions between the gravitational levels can be used to study the properties of neutrons. For instance, if we look for transitions induced by a variable electric field and we establish an upper limit on such transitions, we can establish a limit for the electric charge of the neutron.

6.1 General Expressions for Transition Amplitudes

Let us remind the reader of the main formulas [3] which will be used hereafter concerning the transitions between the quantum levels (two states of the discrete spectrum). We are interested in the transitions induced by a periodical external interaction considered as a perturbation and which, in order to obtain simple analytic expressions, is considered to be harmonic.

The Hamiltonian $\widehat{H}$ of the problem can be written in the form

$$\widehat{H} = \widehat{H_0} + \hat{V}(t) \tag{6.1}$$

where $\widehat{H_0}$ corresponds to the unperturbed gravitational problem $(z > 0)$

$$\widehat{H_0} = \frac{\hat{p}^2}{2m} + mgz \tag{6.2}$$

and

$$\hat{V}(t) = V_0(z)e^{i\omega t} + V_0(z)e^{-i\omega t} \tag{6.3}$$

is a harmonic perturbation with $V_0(z)$ which depends on z. This particular harmonic form of excitation is chosen to obtain analytic results and can in some cases be achieved in an experiment.

A solution Ψ of the Schrödinger equation

$$i\hbar\frac{\partial\Psi}{\partial t} = \left(\widehat{H_0} + \hat{V}(t)\right)\Psi \tag{6.4}$$

can thus be written as a sum

$$\Psi = \sum_k a_k(t)\Psi_k^{(0)} \tag{6.5}$$

over solutions $\Psi_k^{(0)} = \psi_k(z)e^{-iE_k^{(0)}t/\hbar}$ of the unperturbed Schrödinger equation

$$i\hbar\frac{\partial\Psi_k^{(0)}}{\partial t} = \widehat{H_0}\Psi_k^{(0)}. \tag{6.6}$$

If we put (6.5) in (6.4) and taking into account (6.6) we obtain:

$$i\hbar\sum_k \Psi_k^{(0)}\frac{da_k}{dt} = \sum_k a_k\hat{V}(t)\Psi_k^{(0)}. \tag{6.7}$$

By multiplying the last equation by $\Psi_m^{*(0)}$ and by integrating over z, we obtain:

$$i\hbar\frac{da_m}{dt} = \sum_k V_{mk}(t)a_k \tag{6.8}$$

with the matrix element:

$$V_{mk}(t) = \int \Psi_m^{*(0)}\hat{V}(t)\Psi_k^{(0)}dz. \tag{6.9}$$

The last differential equation describes an evolution of the quantum system. If we suppose that at a moment $t = 0$, the system was, for instance, in a ground state ($k = 1$)

$$a_1(0) = 1 \text{ and } a_m(0) = 0 \text{ for any } m \neq 1,$$

then we can calculate, at least numerically, a probability to find the system in the state n for any moment t as

$$P_n(t) = \left|a_n(t)\right|^2. \tag{6.10}$$

As we said previously, the choice of a perturbation interaction $\hat{V}(t)$ in a harmonic form (6.3) allows us to obtain an analytic expression for the probability (6.10) if we consider the problem of only two coupled states. Physically, this situation is produced when the frequency ω of the excitation is close to the difference $\omega_{n0} = (E_n^{(0)} - E_1^{(0)})/\hbar$ (resonance regime). Let us suppose therefore that the difference $\varepsilon = \omega_{n1} - \omega$ is very small and that in the matrix element (6.9) of the perturbation (6.3), we can leave only the dominant term with this small frequency:

$$V_{n1}(t) = \int \Psi_n^{*(0)} \hat{V}(t) \Psi_1^{(0)} dz \approx e^{i\varepsilon t} \int \psi_n^* V_0(z) \psi_1 dz \equiv F_{n1} e^{i\varepsilon t}. \tag{6.11}$$

By omitting all other terms, we obtain a system of two coupled equations relating the amplitudes of presence in the ground and in the *n*-th state:

$$\begin{aligned} i\hbar \frac{da_n}{dt} &= F_{n1} e^{i\varepsilon t} a_1, \\ i\hbar \frac{da_1}{dt} &= F_{n1}^* e^{-i\varepsilon t} a_n. \end{aligned} \tag{6.12}$$

This system can be easily solved, for instance, by the standard Laplace transformation. If we suppose that at $t = 0$ the system is in the ground state, the probability of finding it in the *n*-th excited state appears to be equal to:

$$P_n(t) = \left|a_n(t)\right|^2 = \frac{\Omega_0^2}{\Omega^2} \sin^2 \Omega t \tag{6.13}$$

with

$$\Omega_0 = \frac{F_{n1}}{\hbar} \text{ and } \Omega^2 = \Omega_0^2 + \frac{\varepsilon^2}{4}.$$

This is a well-known Raby formula describing an oscillation of the system between the two coupled states with the frequency 2Ω. The probability of presence in an excited state oscillates between 0 and Ω_0^2/Ω^2.

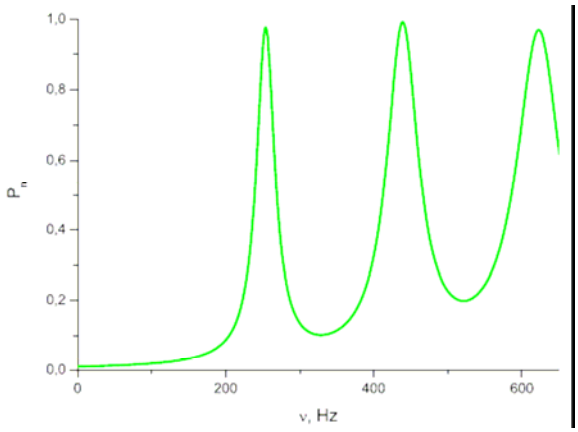

Fig. 13. The transition probability from the ground to the excited states as a function of frequency of a perturbation interaction $\nu = \omega/2\pi$.

The maximum probability as a function of frequency has a resonance-like behavior

$$P_{\max}(\omega) = \frac{\Omega_0^2}{\Omega^2} = \frac{\dfrac{(2F_{n1})^2}{\hbar^2}}{(\omega-\omega_{n1})^2 + \dfrac{(2F_{n1})^2}{\hbar^2}} \tag{6.14}$$

and is presented in Fig. 13. The resonance frequencies given in this figure correspond to transitions from the ground state $n=1$ to the first three excited states. The energy spectrum of the system becomes denser with increasing n (the levels become closer to each other). The width of this resonance is defined by the matrix element of the perturbation F_{n1} and is equal to

$$\Gamma_n = 4F_{n1}. \tag{6.15}$$

To resolve the two nearest states with n and $n+1$, their energy difference $E_{n+1} - E_n = \hbar\omega_{nn+1}$ should be smaller than the corresponding width:

$$\hbar\omega_{nn+1} > \Gamma_n. \tag{6.16}$$

In other words, the matrix element F_{n1} should not be very big

$$F_{n1} < \frac{\hbar\omega_{nn+1}}{4} \tag{6.17}$$

to populate only one excited state.

For an exact resonance $\varepsilon = 0$, formula (6.13) becomes

$$P_n(t) = \sin^2 \Omega_0 t \,. \tag{6.18}$$

For a very small period of time (or a very small matrix element F_{n1}), this probability is seen to depend quadratically on time:

$$P_n(t) \approx \Omega_0^2 t^2 \tag{6.19}$$

(this formula is valid even when not in an exact resonance). We can say that this probability becomes close to 1 if:

$$\frac{F_{n1} t}{\hbar} \approx 1 \,. \tag{6.20}$$

We can say that to have a non-negligible transition probability, the observation time τ should be of the order of:

$$\tau \approx \frac{\hbar}{F_{n1}} \,. \tag{6.21}$$

By combining this condition with the condition of the resolution of two neighboring states (6.17), we conclude that, to observe a resonance transition, the neutron life time in the system should be higher than:

$$\tau > \frac{4}{\omega_{nn+1}} \,. \tag{6.22}$$

For instance, for a transition between the ground state $n = 1$ and first excited state $n = 2$, the corresponding frequency is equal to 254 Hz and we obtain $\tau > 4$ ms. For neighbor higher excited states, this time should be even greater. We would remind the reader that in the last experiment the time of presence of neutron in the system was close to 25 ms.

If the condition (6.22) is not satisfied, the transitions may also occur but in several states simultaneously. This is true in particular, in the case mentioned in the introduction to this chapter: the transition due to the sudden change of the mirror height (negative step). The neutrons from the ground state (before the step) populate a few low excited states (after the step). The transition exists but it is not a resonance one.

6.2 Transitions Induced by a Magnetic Field

As we mentioned at the beginning of this section, the magnetic field $\boldsymbol{B}$ easily couples to the neutron magnetic moment $\hat{\boldsymbol{\mu}}$ by:

$$\hat{H}_{\text{int}} \equiv \hat{V}(t) = -\hat{\boldsymbol{\mu}}\boldsymbol{B} \tag{6.23}$$

and thus can be used to induce transitions between the gravitational levels. To obtain the desirable effect, one can introduce an oscillating magnetic field with a gradient along the *z* axis (which is also the direction of the magnetic field itself):

$$B_z = \beta z \sin \omega t \,. \tag{6.24}$$

For this interaction, the matrix element F_{n1} is equal to:

$$F_{n1} = \mu_{\text{n}} \beta z_{n1} \tag{6.25}$$

where μ_{n} is the neutron magnetic moment and

$$z_{n1} = \int \psi_n^* z \psi_1 dz \,.$$

This matrix element can be calculated numerically with the well-known Airy function and, for instance for $n = 2$, appears to be equal to

$$z_{21} = 0.653 z_0 \tag{6.26}$$

where $z_0 = 5.87\ \mu\text{m}$ is the characteristic length of the problem introduced previously.

This can be easily achieved, even in the current experimental setup. The gradient of the magnetic field β necessary to introduce a transition between the first two levels with a probability close to one (6.20) is equal to:

$$\beta = \frac{\hbar}{\mu_{\text{n}} z_{12} t} \,. \tag{6.26}$$

For the present experiment with $t = 25\ \text{ms}$, we obtain $\beta \approx 10\ \text{Gs/cm}$, which can be achieved without major difficulty. It is planned to conduct this experiment in the very near future.

Let us emphasize that the studies of transitions induced by a magnetic field would represent a very efficient tool for the search for the loss of quantum coherence induced by gravity. The time evolution (6.13) of the two-level system is modified in the presence of such

effects and can be constrained experimentally without any major difficulty. This is another reason why the experiments on magnetic transitions between the gravitational levels are of high priority.

6.3 Transitions Induced by a Gravitational Field

The most interesting transition would be the one induced by gravitational interaction, for instance, by a massive body motion in the vicinity of the setup. Compared to the Coulomb interaction, this process is analogous to an excitation of the Coulomb atom by an electric charge moving near the atom. In a field theory picture, this excitation is induced by a virtual photon. In the case of a transition between the gravitational levels induced by a moving body, one would speak of a virtual graviton. Strictly speaking, the theoretical description of both processes does not require the explicit introduction of these virtual particles. We could not therefore say that the detection of the gravitational transition would be an unambiguous demonstration of the existence of the graviton. Nevertheless, this experiment would be a very important step towards this goal.

The main difficulty is obviously due to the very weak interaction constant. Let us therefore simply estimate the probability of such a transition in order to charge on the feasibility of its observation in the near future, let us say within a decade.

Let us suppose that a transition is induced by an oscillating body moving just above the neutron situated at distance z above the mirror. Thus the distance between the neutron and the body is equal to:

$$r = \frac{L}{2} + a(1-\cos\omega t) + \Delta - z \tag{6.27}$$

where L is the linear size of the body, a is an amplitude of oscillations and Δ is the minimal distance between the body and the mirror. This oscillating body will introduce an additional gravitational interaction:

$$\widehat{H}_{\text{int}} = G\frac{mM}{r} \tag{6.28}$$

M being the mass of the body. z is small with respect to L and this interaction Hamiltonian can be developed in series on z. The linear term is equal to:

$$\widehat{H}_{\text{int}} \approx G\frac{mM}{L}\frac{z}{L}\frac{4}{\left(1+2\zeta(1-\cos\omega t)\right)^2} \tag{6.29}$$

Here Δ is neglected with respect to L and $x = a/L$ is introduced. The function:

$$f(t) = \frac{1}{\left(1+2\zeta(1-\cos\omega t)\right)^2} \tag{6.30}$$

is not harmonic but it is quite easy to calculate its development in Fourier series:

$$f(t)=\sum_{n=-\infty}^{\infty} c_n e^{in\omega t} \tag{6.31}$$

with the coefficients:

$$c_n=\frac{\omega}{2\pi}\int_0^{2\pi/\omega} f(t)e^{-in\omega t}dt=\frac{1}{\zeta\sqrt{1+4\zeta}}\eta^{n+1}\frac{(n+1)-(n-1)\eta^2}{\left(1-\eta^2\right)^2} \tag{6.32}$$

where

$$\eta=1+\frac{1}{2\zeta}-\frac{1}{2\zeta}\sqrt{1+4\zeta}\,. \tag{6.33}$$

As a function of ζ, η increases continuously from 0 to 1.

In particular, the coefficient corresponding to the first harmonic c_1 is equal to:

$$c_1=\frac{2\zeta}{\left(1+4\zeta\right)^{3/2}}\,. \tag{6.34}$$

This coefficient as a function of ζ has a maximum for $\zeta=1/2$ and its maximum value is equal to

$$c_1=0.192\,. \tag{6.35}$$

Let us note that the coefficient describing the difference between the neighbor harmonics is equal to:

$$\eta\left(\zeta=1/2\right)=2-\sqrt{3}\approx 0.268\,. \tag{6.36}$$

This means that the higher terms decrease quite rapidly with *n* and, in first approximation, the interaction (6.30) can be considered as harmonic and can be represented, for the optimal choice $\zeta=1/2$, as:

$$\widehat{H}_{\text{int}}\approx 3.08G\frac{mM}{L}\frac{z}{L}e^{i\omega t}\,. \tag{6.37}$$

This Hamiltonian is now considered as a perturbation $\hat{V}(t)$ and its matrix element F_{21} between the first two states' wave functions is equal to:

$$F_{21} = 0.77G\frac{mM}{L}\frac{z_{21}}{L}, \tag{6.38}$$

where z_{21} is the same as in (6.26).

Obviously, for any realistic experiment, the condition (6.20) will be hardly fulfilled for the gravitational interaction. Even if the neutron life time is chosen as the time of observation (this hypothesis implies successfully storing neutrons at a given gravitational level over a very long period, which is actually an extremely challenging task) and the characteristic size of the oscillating body equals to $L = 20$ cm with high density $\rho = 20 \cdot 10^3$ kg/m^3 (i.e. $M = 160$ kg), the value of the product (6.20) appears to be small:

$$\frac{F_{21}t}{\hbar} \approx 0.01. \tag{6.39}$$

This means that the probability of a corresponding transition would be of the order of 10^{-4}. With existing sources of UCN, the detection of those transitions would scarcely seem possible.

However, the probability of transition increases if we choose other levels, for instance, highly excited neighboring levels. We can show that the matrix element z_{n+1n} behaves, for $n \gg 1$, as:

$$z_{n+1n} \approx 0.57\xi n^{2/3}, \tag{6.40}$$

i.e. increases quite rapidly with *n*, whereas the transition frequency will decrease:

$$\omega_{n+1n} \sim n^{-1/3}. \tag{6.41}$$

Hence the technical realization of the experiment would be even simpler.

Note also that increasing the size *L* of the oscillating body produces very limited gain because the amplitude of the transition depends linearly on *L*: $F_{21} \sim L$, whereas its mass will grow very rapidly $M \sim L^3$ and make the experiment much more complicated.

Taking into account these circumstances, we can conclude that an experimental observation of a transition between two gravitational levels, induced by the motion of a body seems relatively unlikely in the near future with the existing neutron sources.

6.4 Transitions Induced by an Electrical Field

By studying transitions between the levels induced by an oscillating electric field, we can establish an upper limit on (or find) the neutron charge.

As an example, let us consider a system where the mirror is one of the plates of a condenser. If we apply a varying electric field a perturbation Hamiltonian:

$$\widehat{H}_{\text{int}} \equiv \widehat{V}(t) = e_{\text{n}} E e^{i\omega t} z \tag{6.42}$$

e_{n} being the neutron charge, E the strength of the electric field.

For this interaction, the matrix element F_{n1} is equal to:

$$F_{n1} = e_{\text{n}} E z_{n1}. \tag{6.43}$$

Thus an upper limit for the probability of transition to the nth state P_{lim} will give an upper limit on the neutron charge:

$$e_{\text{n}} < \frac{\hbar}{E z_{n1} t} \sqrt{P_{\text{lim}}}\ . \tag{6.44}$$

In an experiment with the electric field $E \approx 10^7$ V/m, with t compatible with the neutron life time, $P_{\text{lim}} \approx 10^{-3}$ must be achieved in order to obtain an actual limit on the neutron electric charge equal to $e_{\text{n}} < 10^{-21} e$. The best limit is produced with the interferometer experiment using very cold neutrons [62]. It should be noted that ultracold neutrons were also used to establish the limit [63].

6.5 Transitions Induced by the Combined Effect of Different Excitations

Nevertheless a much tighter constraint for the neutron electric charge can be obtained and a transition induced by a moving massive body can be observed experimentally. The idea is to conduct an interference experiment where we measure a transition induced by two different causes, for instance, by a variable gradient of the magnetic field and a varying electric field or an oscillating body.

The matrix element F_{nk} of such a transition would be equal to the sum:

$$F_{nk} = F_{nk}^{\text{big}} + F_{nk}^{\text{small}} \tag{6.45}$$

of a big F_{nk}^{big} (for instance, magnetic) and a small F_{nk}^{small} (electric or gravitational) terms. The transition probability would be proportional to:

$$P_+(t) \sim \left|F_{nk}\right|^2 \approx \left|F_{nk}^{\text{big}}\right|^2 + 2F_{nk}^{\text{small}}F_{nk}^{\text{big}}. \quad (6.46)$$

By an adequate choice of the relative phase of these two perturbations, we can obtain another probability:

$$P_-(t) \sim \left|F_{nk}^{\text{big}}\right|^2 - 2F_{nk}^{\text{small}}F_{nk}^{\text{big}}. \quad (6.47)$$

Thus, an asymmetry is proportional to:

$$A = \frac{P_+(t) - P_-(t)}{P_+(t) + P_-(t)} \approx 2\left|\frac{F_{nk}^{\text{small}}}{F_{nk}^{\text{big}}}\right|. \quad (6.48)$$

With the estimation obtained previously (6.39), this kind of measurement seems to be conceivable in future experiments.

Of course, exactly the same idea of combined perturbations can be used to improve the limit on the neutron electric charge.

Conclusion

Gravitationally bound quantum states of neutrons were recently discovered in the measurement of neutron transmission through a narrow horizontal slit between a mirror below and an absorber/scatterer above it. The first experiment allowed us to identify clearly the ground quantum state in this system [12, 13]. Later, with improved height (energy) resolution and statistics, we were also able to measure also the first excited quantum state [15]. We showed that the process of the loss of neutrons in an absorber/scatterer could be very precisely described using a model of neutron tunneling through the gravitational barrier between the classically allowed height and the absorber/scatterer height [15]. Further progress with this experiment using the flow-through measuring mode is limited to a large degree by one fundamental factor: the finite sharpness of the dependence on height of neutron tunneling through this gravitational barrier. Nevertheless, with a more suitable and precise theoretical description [18] and improvements to the absolute distance calibration [19, 20], we can expect to achieve a few percent accuracy in the determination of quantum state parameters.

In order to resolve higher excited quantum states clearly and measure their parameters accurately, we investigate another method based on position-sensitive neutron detectors of very high spatial resolution [21, 22]. The direct measurement of the spatial density distribution in a standing wave is preferred to its investigation with the aid of an absorber/scatterer whose height can be adjusted. The former technique is differential, since it permits the simultaneous measurement of the probability that neutrons reside at all heights of interest. The latter technique is integral, since the information on the probability that neutrons reside at a given height is in fact obtained by the subtraction of the values of neutron fluxes measured for two close values of the scatterer height. Clearly, the differential technique is much more statistically sensitive. Furthermore, the scatterer employed in the integral

technique inevitably distorts the measured quantum states; the finite accuracy of taking these distortions into account results in methodological errors and ultimately limits the attainable accuracy of the measurement of the quantum state parameters. The feasibility of the differential technique was demonstrated in refs. [15, 23].

The two techniques considered and the available fluxes of UCN are already sufficient for a broad range of applications. Thus, as this was shown in ref. [24], this experiment could be used to establish a competitive limit for short-range fundamental forces. However, it is from other specially designed neutron experiments that further progress in the nanometer range of distances can be expected. In order to be competitive in the micrometer range, we have to improve accuracy by many orders of magnitude, which can only be possible using the technique of resonance transitions between the quantum states. This experiment can also be used to search for the axion – a hypothetical particle which strongly violates CP-invariance; the characteristic distance for this interaction should be comparable to the characteristic length of our problem z_0. The very fact that the neutron quantum states exist provides the best constraint at this distance. An improvement by many orders of magnitude would seem to be easily achievable. This method could also be used for studies related to the foundations of quantum mechanics, such as for instance, quantum-mechanical localization (revivals phenomenon) or various extensions of quantum mechanics. For instance, it could be used to clearly rule out, or confirm, the presence of the logarithmic term in the Schrödinger equation in some models. It should be also noted that the present method provides two unique opportunities: on the one hand, it provides a rare combination of quantum states and gravitation that is favorable for testing possible extensions of quantum mechanics; on the other hand, UCN can be reflected from the surface $\sim 10^5$ times without loss, i.e. much more than for optical phenomena, which means that any kind of localization can be better studied with UCN. Finally, this method could be very useful for such problems of high interest as the fundamental loss of quantum coherence in systems with gravitational interaction.

Other methodological applications of the gravitationally bound quantum states and related techniques lie outside the subject of the present discussion of quantum gravity phenomena. We will therefore not discuss them in detail but simply mention a number of them. These experiments helped us to find an alternative approach to the problem of the neutron-tight valve for UCN traps able to operate in the broad range of temperatures needed for precision experiments with UCN storage. This is of crucial importance for precision neutron lifetime experiments. The existing solutions suffer from highly disturbing side effects: the so-called gravitational valve [64] modifies the spectrum of the stored UCN, whereas the so-called liquid valve [65,66] means the unavoidable use of fomblin oil with the accompanying effect of quasi-elastic scattering [67,68], producing large false effects also. Other methodological applications include the possibility of studying the distribution of hydrogen above/below solid or liquid surfaces, or the investigation of thin film on surfaces. These two subjects will be considered in more detail in separate publications.

A qualitatively new step in accuracy could be achieved even with the existing UCN density if the resonance transitions between the gravitationally bound quantum states were observed. These transitions could be initiated in various ways and by different forces (strong, electromagnetic, gravitational). In this article we presented for the first time a feasibility analysis and theoretical description of the observation of resonance transitions between the quantum states. All the above-mentioned applications of gravitationally bound quantum states

for various physical problems would benefit considerably from the increase in accuracy which the technique of resonance transitions could bring. Moreover, a new class of highly competitive experiments could be considered, such as better constraints for the electric neutrality of neutrons, or the resonance transitions between the quantum states due to the gravitational interaction. It is clear that any increase in the energy resolution in measurements of the resonance transitions between the quantum states requires a high density of UCN. We therefore consider new approaches in order for significantly increasing the UCN densities, such as the thermalization of neutrons in gels of ultracold nanoparticles [69].

Acknowledgements

The experiments presented here were carried out by a dynamic and enthusiastic collaboration involving, at different stages, H. Abele, S. Baeßler, T.A. Baranova, H.G. Börner, G. Divkovic, A.M. Gagarski, T.M. Kuzmina, L. Lucovac, S. Nahrwold, G.A. Petrov, A.K. Petukhov, S. Raeder, F.J. Rueß, J. Schrauwen, S.M. Soloviev, T. Stöferle, A.V. Strelkov, V.G. Tishchenko, A.Yu. Voronin and A. Westphal, as well as the authors of the present article. We all benefited enormously from discussions with the advice help and support of K. Ben-Saidane, D. Berruyer, Th. Brenner, J. Butterworth, R. Corner, F. Descamps, D. Dubbers, E. Engel, N.P. Filatov, P. Geltenbort, B. Gerard, N. Havercamp, A. Hillairet, M. Jentschel, P. van Isaker, A.G. Kharitonov, C. Krantz, A.J. Leadbetter, A. Lensch, E.V. Lychagin, J.F. Marchand, D. Mund, A.Yu. Muzychka, R. Onofrio, B.G. Peskov, S.V. Pinaev, S. Roccia, V.A. Rubakov, R. Rusnyak, M.E. Shaposhnikov, I.A. Snigireva, E. Tomasi-Gustafson, S. Tinniswood, P.G. Tinyakov, J.-P. Varini, A.A. Zhdanov and M. Zimer.

References

[1] Breit, G. *Phys. Rev*.1928, 32, 273.
[2] Goldman, I.I.; Krivchenkov, V.D.; Kogan, V.I.; Galitsci, V.M. *Problems in Quantum Mechanics*; Academic Press: New York, 1960.
[3] Landau, L.D.; Lifshits, E.M. *Quantum Mechanics*; Pergamon Press: Oxford, 1977.
[4] Flügge, S. *Practical Quantum Mechanics*; Springer-Verlag: Berlin, 1974; Vol. 1.
[5] ter Haar, D. *Selected Problems in Quantum Mechanics*; Academic Press: New York, 1964.
[6] Sakurai, J.J. *Modern Quantum Mechanics*; Benjamin/Cummings: Menlo Park, 1985.
[7] Galitzky, V.M.; Karnakov, B.M.; Kogan, V.I. *La mécanique quantique. Problèmes résolus* EDP Sciences: Les Ulis, 2002; Vol. 1; 2003 ; Vol. 2.
[8] Luschikov, V.I. *Physics Today* 1977, 42, 51.
[9] Luschikov, V.I.; Frank, A.I*.; JETP Lett.* 1978, 28, 559.
[10] Golub, R.; Richardson, D.J.; Lamoreux, S.K. Ultracold Neutrons; Higler: Bristol, 1991.
[11] Ignatovich, V. K. *The Physics of Ultracold Neutrons*; Clarendon: Oxford, 1990.
[12] Nesvizhevsky, V.V.; Börner, H.G.; Petoukhov, A.K.; Abele, H.; Bäßler, S.; Rueß, F.J.; Stöferle, Th.; Westphal, A.; Gagarski, A.M.; Petrov, G.A.; Strelkov, A.V. *Nature* 2002, 415, 297.

[13] Nesvizhevsky, V.V.; Börner, H.G.; Gagarski, A.M.; Petoukhov, A.K.; Petrov, G.A.; Abele, H.; Bäßler, S.; Divkovic, G.; Rueß, F.J.; Stöferle, Th.; Westphal, A.; Strelkov, A.V.; Protasov, K.V.; Voronin, A.Yu. *Phys. Rev*. 2003, D67, 102002-1.
[14] Nesvizhevsky, V.V.; Petoukhov, A.K.; Börner, H.G.; Protasov, K.V.; Voronin, A.Yu.; Westphal, A.; Bäßler, S.; Abele, H.; Gagarski, A.M. *Phys. Rev*. 2003, D68, 108702.
[15] Nesvizhevsky, V.V.; Petoukhov, A.K.; Börner, H.G.; Baranova, T.A.; Gagarski, A.M.; Petrov, G.A.; Protasov, K.V.; Voronin, A.Yu.; Bäßler, S.; Abele, H.; Westphal, A.; Lucovac, L. to appear in *Eur.Phys.J. C*, 2005; (2005). Study of the neutron quantum states in the gravity field. hep-ph/0502081.
[16] Rauch H.; Werner, S. Neutron Interferometry; Oxford University: New York, 2000.
[17] Nesvizhevsky, V.V. *Phys. Usp.* 2004, 46, 93 [Uspekhi Fizicheskikh Nauk 2004, 146, 102].
[18] Voronin, A.Yu.; et al., to be published.
[19] Schrauwen,V. Diploma thesis, UGent, Belgium, 2004.
[20] Nesvizhevsky, V.V.; et al., to be published.
[21] Nesvizhevsky, V.V.; Börner, H.G.; Gagarski, A.M.; Petrov, G.A.; Petoukhov, A.K.; Abele, H.; Bäßler, S.; Stöferle, Th.; Soloviev, S.M. *Nuclear Instruments and Methods in Physics Research* 2000, A440, 754.
[22] Nesvizhevsky, V.V. *Phys. Usp.* 2004, 47, 515 [Uspekhi Fizicheskikh Nauk 2003, 147, 569].
[23] Nesvizhevsky, V.V.; Börner, H.G.; Petoukhov, A.K.; Gagarski, A.M.; Petrov, G.A.; Lukovac, L.; Abele, H.; Wahrwold, S.; Baeßler, S.; Raeder, S.; Kuzmina, T.M.; Schrauwen, J.; Tischenko, V.M.; Protasov, K.V.; Voronin, A.Yu. *ILL Annual Report* 2004.
[24] Nesvizhevsky, V.V.; Protasov, K.V.; *Class. Quant. Grav*. 2004, 21, 4557.
[25] Robinett, R.W. *Phys. Rep.* 2004, 392, 1
[26] Steyerl, A.; Malik, S.S. *Ann. Phys.* 1992, 217, 222.
[27] Steyerl, A.; Malik, S.S. *Phys. Lett.* 1996, A217, 194.
[28] Ellis, J.; Hagelin, J.S.; Nanopoulos, D.V.; Srednicki, M. *Nucl. Phys*. 1984, B241, 381.
[29] Mavromatos, N. (2004). CPT Violation and decoherence in quantum gravity. gr-qc/0407005.
[30] Murayama, H.; Raffelt, G. Hagmann, C.; van Bibber, K.; Rosenberg, L.J. Review of Particle Physics, *Phys. Lett*. 2004, B592, 389.
[31] Arkani-Hamed, N.; Dimopoulos, S.; Dvali, G. *Phys. Lett*. 1998*,* B429, 263;
[32] Arkani-Hamed, N.; Dimopoulos, S.; Dvali, G. *Phys. Rev*. 1999, D59, 086004;
[33] Antoniadis, I.; Arkani-Hamed, N.; Dimopoulos, S.; Dvali, G. *Phys. Lett*. 1998, B436, 257
[34] Rubakov, V.A.; Shaposhnikov, M.E. *Phys. Lett*. 1983, B125, (1983) 136;
[35] Rubakov, V.A.; Shaposhnikov, M.E. *Phys. Lett*. 1983, B125, (1983) 139.
[36] Visser, M. *Phys. Lett*. 1985, B159, 22.
[37] Antoniadis, I. *Phys. Lett*. 1990, B246, 377.
[38] Lykken, J. *Phys. Rev*. 1996, D54, 3693.
[39] Hewett, J.; March-Russell, J. Review of Particle Physics, *Phys. Lett*. 2004, B592, 1056.
[40] Adelberger, E.G.; Heckel, B.R.; Nelson, A.E. *Ann. Rev. Nucl. Part. Sci*. 2003, 53, 77.

[41] Bordag, M.; Mohideen, U.; Mostepanenko, V.M. *Phys. Rep.* 2001, 353, 1;
[42] Mostepanenko, V.M. In The Gravitational Constant: Generalized Gravitational Theories and Experiments; de Sabbaata, V.; Gilles, G.T.; Melnikov, V.N.; Eds.; *NATO Sciences Series*, Kluwer: Dordrecht, 2004; p. 269.
[43] Carugno, G.; Fontana, Z.; Onofrio, R.; Rizzo, C. *Phys. Rev*. 1997, D55, 6591;
[44] Bressi, G.; Carugno, G.; Galavni, A.; Onofrio, R.; Ruoso, G. Class. *Quant. Grav*. 2000, 17, 2365;
[45] Bressi, G.; Carugno, G.; Galavni, A.; Onofrio, R.; Ruoso, G.; Veronese, F. *Class*. *Quant. Grav*. 2001, 18, 3943;
[46] Bressi, G.; Carugno, G.; Galavni, A.; Onofrio, R.; Ruoso, G. *Phys. Rev. Lett*. 2004, 88, 041804.
[47] Long, J.C.; Chan, H.W.; Price, J.C. *Nucl. Phys*. 1999, B539, 23.
[48] Frank, A.; van Isaker, P.; Gomes-Camacho*, J. Phys. Lett*. 2004, B582, 15.
[49] Bertolami, O.; Nunes, F.M.; Class. *Quant. Grav*. 2003, 20, L61.
[50] Abele, H.; Westphal, A. Quantum states of neutrons set limits for non-Newtonian interaction, *ILL Annual Report* 2002, 76;
[51] Abele, H.; Baessler, S.; Westphal, A. *Lect. Notes Phys*. 2003, 631, 355.
[52] Hory, M.; Eades, J.; Hayano, R.S.; Ishikawa, T.; Sakaguchi, J.; Widmann, E.; Yamaguchi, H.; Torii, H.A.; Juhász, B.; Horváth, D.; Yamazaki, T. *Phys. Rev. Lett*. 2003, 91, 123401
[53] Korobov, V.I. *Phys. Rev.* 2003, A67, 062501;
[54] Korobov, V.I. *Phys. Rev*. 2003, A68, 019902 (erratum).
[55] Watson, P. (2004). A limit on short-range modifications of gravity. hep-ph/0406308.
[56] Kolb, E. W.; Turner, M.S. The Early Universe; Addison-Wesley: Redwood, CA, 1990.
[57] Moody J. E.; Wilczek, F. Phys. Rev. 1984, D30, 130.
[58] Rosenberg, L. J. In Proceedings of the Workshop on Particle and Nuclear Astrophysics in the Next Millennium, Snowmass; World Scientific: Singapore, 1994.
[59] Youdin, A.N.; Krause, Jr., D.; Jagannathan, K.; Hunter, L.R.; Lamoreaux, S.K. *Phys. Rev. Lett.* 1996, 77, 2170.
[60] Wei-Tou Ni; Sheau-shi Pan; Hsien-Chi Yeh; Li-Shing Hou; Juling Wan. *Phys. Rev. Lett.* 1999, 82, 2439.
[61] Kobzarev, I.Yu.; Okun, L.B. Sov. Phys. JETP 1963, 16, 1343 [*Zh. Exp. Teor. Phys.* 1962, 43, 1904.]
[62] Leitner, J.; Okubo, S. *Phys. Rev*. 1964, 136, 1542.
[63] Mashhoon, B. Class. *Quant. Grav.* 2000, 17, 2399.
[64] Obukhov, Yu.N. Phys. *Rev. Lett*. 2001, 86, 192.
[65] Bini, D.; Cherubini, Ch.; Mashhoon, B. *Class. Quant. Grav*. 2004, 21, 3893.
[66] Alfimenkov, V.P.; Strelkov, A.V.; Shvetsov, V.N.; Nesvizhevsky, V.V.; Serebrov, A.P.; Tal'daev, R.R.; Kharitonov, A.G. *JETP Lett.* 1992, 55, *84 [Pis'ma Zh. Eksp. Teor. Fiz*. 1992, 55, 92].
[67] Steyerl, A.; Malik, S.S.; Geltenbort, P.; Neumaier, S.; Nesvizhevsky, V.V.; Utsuro, M.; Kawabata, Y. *Journal de Physique III* 1997, 7, 1941.
[68] Bestle, T.; Geltenbort, P.; Just, H.; Kawabata, Y.; Malik, S.S.; Nesvizhevsky, V.V.; Neumaier, S.; Okumura, K.; Steyerl, A.; Utsuro, M. *Phys. Lett.* 1998, A244, 217.

[69] Nesvizhevsky, V.V. To appear in Int. *J. Mod. Phys. D*; (2005) Constraints for quasi-elastic neutron reflections in the range $dE \sim 10^{-12} - 10^{-13}$ eV. nucl-th/0502023.
[70] Collela, R.; Overhauser, A.W.; Werner, S.A. *Phys. Rev. Lett*. 1975, 34, 1472.
[71] Baumann, J.; Gähler, R.; Kalus, J.; Mampe, W. *Phys. Rev*. 1988, D37, 3107.
[72] Borisov, Yu.V.; Borovikova, N.V.; Vasilyev, A.V.; Grigorieva, L.A.; Ivanov, S.N.; Kashukeev, N.T.; Nesvizhevsky, V.V.; Serebrov, A.P.; Yaidjiev, P.S. *J. Tech. Phys.* 1988, 58 *[Zh. Tech. Fiz*. 1988, 58, 951].
[73] Nesvizhevsky, V.V.; Serebrov, A.P.; Tal'daev, R.R.; Kharitonov, A.G.; Alfimenkov, V.P.; Strelkov, A.V.; Shvetsov, V.N. Sov. *Phys. JETP* 1992, 75, 405. [*Zh. Eksp. Teor. Fiz*. 1992, 102, 740].
[74] Mampe, W.; Ageron, P.; Bates, C.; Pendlebury, J.M.; Steyerl, A. *Phys. Rev. Lett*. 1989, 63, 593.
[75] Arzumanov, S.; Bondarenko, L.; Chernyavsky, S.; Drexel, W.; Fomin, A.; Geltenbort, P.; Morozov, V.; Panin, Yu.; Pendlebury, J.; Schreckenbach, K. *Phys. Lett*. 2000, B483, 15.
[76] Nesvizhevsky, V.V.; Strelkov, A.V.; Geltenbort, P.; Iaydjiev, P.S. *Eur. J. Appl. Phys*. 1999, 6, 151;
[77] Bondarenko, L.N.; Geltenbort, P.; Korobkina, E.I.; Morozov, V.I.; Panin, Yu.N. *Phys. At. Nucl*. 2002, 65, 11 [*Yad. Fiz*. 2002, 65, 11]
[78] Nesvizhevsky, V.V. *Phys. At. Nucl*. 2002, 65, 400 [*Yad. Fiz*. 2002, 65, 426].